Bioactivities of Phenalenones

Subjects: Biotechnology & Applied Microbiology
Contributor: Sabrin R. M. Ibrahim , Abdelsattar M. Omar , Yosra A. Muhammad , Ali A. Alqarni , Abdullah M. Alshehri , Shaimaa G. A. Mohamed , Hossam M. Abdallah , Mahmoud A. Elfaky , Gamal A. Mohamed , Jianbo Xiao

Phenaloenones are structurally unique aromatic polyketides that have been reported in both microbial and plant sources. They possess a hydroxy perinaphthenone three-fused-ring system and exhibit diverse bioactivities, such as cytotoxic, antimicrobial, antioxidant, and anti-HIV properties, and tyrosinase, α-glucosidase, lipase, AchE (acetylcholinesterase), indoleamine 2,3-dioxygenase 1, angiotensin-I-converting enzyme, and tyrosine phosphatase inhibition. They have a rich nucleophilic nucleus that has inspired many chemists and biologists to synthesize more of these related derivatives.

phenalenones fungi bioactivities

1. Introduction

In the last few decades, fungi have attracted tremendous scientific attention due to their capability to biosynthesize diverse classes of bio-metabolites, with varied bioactivities that are utilized for pharmaceutical, medicinal, and agricultural applications [1][2][3][4][5][6][7][8][9][10][11][12][13][14]. Obviously, the number of reported biometabolites from a fungal origin is rapidly growing [15][16][17][18][19]. Fungi can produce a wide variety of structurally unique polyketide-derived metabolites; among them are phenalenones, in which various post-modifications, including prenylation, transamination, rearrangement, and oxidation diversify their structures [20][21][22]. Phenalenones belong to the aromatic ketones, consisting of a hydroxyl-perinaphthenone three-fused-ring system that has been reported as from both microbial and plant sources [21]. They are recognized as the higher plants' phytoalexins, which confer resistance toward pathogens [23][24]. Phenalenones are also known as pollutants, resulting from the combustion of fossil fuels [21]. The first report of the isolation of a phenalenone derivative from a fungal source was in 1955 [25][26]. Fungal phenalenones have immense structural diversity, such as hetero- and homo-dimerization, and high degrees of nitrogenation and oxygenation, as well as the capacity to be complexed with metals, incorporating additional carbon frameworks or an isoprene unit by the formation of either a linear ether or a trimethyl-hydrofuran moiety [20][21]. Moreover, many acetone adducts of phenalenones were also reported that have an extended carbon chain at ring A, such as the acyclic diterpenoid adducts. These fungal metabolites have been demonstrated to exhibit a wide range of bioactivities, such as cytotoxic, antimicrobial, antioxidant, and anti-HIV, and tyrosinase, α-glucosidase, lipase, AchE (acetylcholinesterase), indoleamine 2,3-dioxygenase 1, angiotensin-I-converting enzyme, and tyrosine phosphatase inhibition. They are of great interest as potential lead compounds for synthetic organic chemistry because of the stability of their anions, phenalenyl radicals, and cations, as well as their interesting photophysical properties [27][28][29].

2. Biological Activities of Phenalenones

The bioactivities of some of the reported metabolites have been investigated. In this regard, 70 metabolites have been associated with some type of biological action, including cytotoxic, antimalarial, antimycobacterial, anti-inflammatory, anti-angiogenic, immunosuppressive, and antioxidant properties, as well as IDO1, α-glucosidase (AG), ACE, tyrosinase, and PTP inhibition. This information has been discussed and listed in **Table 1**.

Table 1. Biological activities of the most active fungal phenalenones.

Compound Name	Biological Activity	Assay, Organism, or Cell Line	Biological Results	Positive Control	Ref.
Paecilomycone A (**1**)	Tyrosinase inhibition	Colorimetric-microtiter plates/Tyrosinase enzyme	0.11 mM (IC_{50})	Kojic acid 0.10 mM (IC_{50}) Arbutin 0.20 mM (IC_{50})	[30]
Paecilomycone B (**2**)	Tyrosinase inhibition	Colorimetric-microtiter plates/Tyrosinase enzyme	0.17 mM (IC_{50})	Kojic acid 0.10 mM (IC_{50}) Arbutin 0.20 mM (IC_{50})	[30]
Paecilomycone C (**3**)	Tyrosinase inhibition	Colorimetric-microtiter plates/Tyrosinase enzyme	0.14 mM (IC_{50})	Kojic acid 0.10 mM (IC_{50}) Arbutin 0.20 mM (IC_{50})	[30]
Aspergillussanone A (**5**)	Cytotoxicity	Resazurin microplate/KB	48.4 μM (IC_{50})	Ellipticine 4.1 μM (IC_{50})	[31]
		Resazurin microplate/Vero	34.2 μM (IC_{50})	Ellipticine 4.5 μM (IC_{50})	[31]
ent-Peniciherqueinone (**8**)	Adipogenesis induction	Adiponectin production assay/hBM-MSC(B7)	57.5 μM (IC_{50})	Pioglitazone 0.69 μM (IC_{50})	[32]
Herqueinone (**9**)	Antioxidant	DPPH/$DPPH^{\bullet}$	0.48 mM (IC_{50})	Butylated hydroxytoluene 0.11 mM (IC_{50})	[33]
		Hydroxyl radical scavenging/$OH^{\bullet}$	6.34 mM (IC_{50})	Tannic acid 0.26 mM (IC_{50})	[33]
		Superoxide radical scavenging/$O_2^{\bullet-}$	4.11 mM (IC_{50})	Trolox 0.96 mM (IC_{50})	[33]
Isoherqueinone (**12**)	Adipogenesis induction	Adiponectin production assay/hBM-MSC(B7)	39.7 μM (IC_{50})	Pioglitazone 0.69 μM (IC_{50})	[32]
Acetone adduct of a	Anti-	Nitric oxide synthase/RAW	3.2 μM	AMT 0.2 μM	[32]

Compound Name	Biological Activity	Assay, Organism, or Cell Line	Biological Results	Positive Control	Ref.
triketone (**17**)	inflammatory	264.7	(IC_{50})	(IC_{50})	
(+)-Sclerodin (**21**)	Cytotoxicity	SRB/U87MG	55.99 µM (IC_{50})	Doxorubicin 1.2 µM (IC_{50})	[34]
		SRB/C6	44.65 µM (IC_{50})	Doxorubicin 0.47 µM (IC_{50})	[34]
(−)-Sclerodinol (**24**)	Antimicrobial	Agar dilution/*B. cereus*	25.0 µM (MIC)	Ciprofloxacin 0.39 µM (MIC)	[35]
		Agar dilution/*Proteus* species	50.0 µM (MIC)	Ciprofloxacin 0.78 µM (MIC)	[35]
		Agar dilution/*M. Phlei*	25.0 µM (MIC)	Ciprofloxacin 0.39 µM (MIC)	[35]
		Agar dilution/*B. subtilis*	12.5 µM (MIC)	Ciprofloxacin 0.39 µM (MIC)	[35]
		Agar dilution/*V. parahemolyticus*	12.5 µM (MIC)	Ciprofloxacin 0.39 µM (MIC)	[35]
		Agar dilution/MRCNS	50.0 µM (MIC)	Ciprofloxacin 25.0 µM (MIC)	[35]
		Agar dilution/MRSA	50.0 µM (MIC)	Ciprofloxacin > 50 µM (MIC)	[35]
Bipolarol C (**26**)	Antibacterial	REMA/*B. cereus*	25.0 µg/mL (MIC)	Vancomycin 1.0 µg/mL (MIC)	[36]
4-Hydroxysclerodin (**27**)	Anti-angiogenetic	Tube formation assay/HUVECs	20.9 µM (IC_{50})	Sunitinib 1.5 µM (IC_{50})	[32]
(+)-Sclerodione (**28**)	Cytotoxicity	SRB/U87MG	60.93 µM (IC_{50})	Doxorubicin 1.2 µM (IC_{50})	[34]
		SRB/C6	60.81 µM (IC_{50})	Doxorubicin 0.47 µM (IC_{50})	[34]
	Antibacterial	Micro-broth dilution/MRSA	23.0 µg/mL (MIC)	Gentamicin 0.5 µg/mL (MIC)	[34]

Compound Name	Biological Activity	Assay, Organism, or Cell Line	Biological Results	Positive Control	Ref.
		Micro-broth dilution/*E. coli*	35.0 µg/mL (MIC)	Gentamicin 1.0 µg/mL (MIC)	[34]
(−)–Sclerodione (**29**)	α-Glucosidase inhibition	Colorimetric/α-Glucosidase	120 µM (IC_{50})	N-deoxynojirimycin 130.5 µM (IC_{50})	[37]
	Porcine-lipase inhibition	Colorimetric/Porcine lipase	1.0 µM (IC_{50})	Orlistat 9.4 µM (IC_{50})	[37]
(−)-Bipolaride B (**30**)	Antibacterial	REMA/*B. cereus*	25.0 µg/mL (MIC)	Vancomycin 1.0 µg/mL (MIC)	[36]
	Cytotoxicity	REMA/MCF-7	79.4 µM (IC_{50})	Doxorubicin 12.99 µM (IC_{50}) Tamoxifen 19.39 µM (IC_{50})	[36]
		REMA/KB	96.8 µM (IC_{50})	Ellipticine 8.32 µM (IC_{50}) Doxorubicin 1.15 µM (IC_{50})	[36]
		REMA/NCI-H187	56.5 µM (IC_{50})	Ellipticine 9.74 µM (IC_{50}) Doxorubicin 0.19 µM (IC_{50})	[36]
Peniciphenalenin H (**31**)	Antimicrobial	Agar dilution/*Proteus* species	50.0 µM (MIC)	Ciprofloxacin 0.78 µM (MIC)	[35]
		Agar dilution/*B. subtilis*	25.0 µM (MIC)	Ciprofloxacin 0.39 µM (MIC)	[35]
		Agar dilution/*V. parahemolyticus*	25.0 µM (MIC)	Ciprofloxacin 0.39 µM (MIC)	[35]
		Agar dilution/MRCNS	25.0 µM (MIC)	Ciprofloxacin 25.0 µM (MIC)	[35]
		Agar dilution/MRSA	50.0 µM (MIC)	Ciprofloxacin > 50 µM (MIC)	[35]
Bipolarol A (**32**)	Cytotoxicity	REMA/MCF-7	110.4 µM (IC_{50})	Doxorubicin 12.99 µM (IC_{50})	[36]

Compound Name	Biological Activity	Assay, Organism, or Cell Line	Biological Results	Positive Control	Ref.
				Tamoxifen 19.39 μM (IC_{50})	
(+)-Scleroderolide (**33**)	Cytotoxicity	SRB/U87MG	37.26 μM (IC_{50})	Doxorubicin 1.2 μM (IC_{50})	[34]
		SRB/C6	23.24 μM (IC_{50})	Doxorubicin 0.47 μM (IC_{50})	[34]
	Antibacterial	Micro-broth dilution/MRSA	7.0 μg/mL (MIC)	Gentamicin 0.5 μg/mL (MIC)	[34]
		Micro-broth dilution/*E. coli*	9.0 μg/mL (MIC)	Gentamicin 1.0 μg/mL (MIC)	[34]
(−)–Scleroderolide (**34**)	α-Glucosidase inhibition	Colorimetric/α-Glucosidase	48.7 μM (IC_{50})	*N*-Deoxynojirimycin 130.5 μM (IC_{50})	[37]
	porcine-lipase inhibition	Colorimetric/Porcine lipase	3.4 μM (IC_{50})	Orlistat 9.4 μM (IC_{50})	[37]
(−)-Bipolaride A (**36**)	Antibacterial	REMA/*B. cereus*	12.5 μg/mL (MIC)	Vancomycin 1.0 μg/mL (MIC)	[36]
	Cytotoxicity	REMA/NCI-H187	60.2 μM (IC_{50})	Ellipticine 9.74 μM (IC_{50}) Doxorubicin 0.19 μM (IC_{50})	[36]
(−)-Bipolaride E (**39**)	Antibacterial	REMA/*B. cereus*	12.5 μg/mL (MIC)	Vancomycin 1.0 μg/mL (MIC)	[36]
	Cytotoxicity	REMA/MCF-7	65.1 μM (IC_{50})	Doxorubicin 12.99 μM (IC_{50}) Tamoxifen 19.39 μM (IC_{50})	[36]
		REMA/KB	94.4 μM (IC_{50})	Ellipticine 8.32 μM (IC_{50}) Doxorubicin 1.15 μM (IC_{50})	[36]

Compound Name	Biological Activity	Assay, Organism, or Cell Line	Biological Results	Positive Control	Ref.
		REMA/NCI-H187	86.9 μM (IC_{50})	Ellipticine 9.74 μM (IC_{50}) Doxorubicin 0.19 μM (IC_{50})	[36]
Bipolarol B (**40**)	Cytotoxicity	REMA/MCF-7	65.3 μM (IC_{50})	Doxorubicin 12.99 μM (IC_{50}) Tamoxifen 19.39 μM (IC_{50})	[36]
		REMA/KB	52.5 μM (IC_{50})	Ellipticine 8.32 μM (IC_{50}) Doxorubicin 1.15 μM (IC_{50})	[36]
		REMA/NCI-H187	48.3 μM (IC_{50})	Ellipticine 9.74 μM (IC_{50}) Doxorubicin 0.19 μM (IC_{50})	[36]
Bipolarol D (**41**)	REMA/MCF-7	REMA/MCF-7	108.7 μM (IC_{50})	Doxorubicin 12.99 μM (IC_{50}) Tamoxifen 19.39 μM (IC_{50})	[36]
(−)-Bipolaride C (**42**)	Antibacterial	REMA/*B. cereus*	12.5 μg/mL (MIC)	Vancomycin 1.0 μg/mL (MIC)	[36]
	Cytotoxicity	REMA/MCF-7	48.9 μM (IC_{50})	Doxorubicin 12.99 μM (IC_{50}) Tamoxifen 19.39 μM (IC_{50})	[36]
		REMA/KB	34.4 μM (IC_{50})	Ellipticine 8.32 μM (IC_{50}) Doxorubicin 1.15 μM (IC_{50})	[36]
		REMA/NCI-H187	59.8 μM (IC_{50})	Ellipticine 9.74 μM (IC_{50}) Doxorubicin 0.19 μM (IC_{50})	[36]
		REMA/Vero	53.1 μM (IC_{50})	Ellipticine 2.13 μM (IC_{50})	[36]
Flaviphenalenone A (**45**)	Cytotoxicity	MTT/A549	6.6 μg/mL	Doxorubicin HCl 0.2 μg/mL (IC_{50})	[38]

Compound Name	Biological Activity	Assay, Organism, or Cell Line	Biological Results	Positive Control	Ref.
			(IC_{50})		
		MTT/MCF-7	10.0 µg/mL (IC_{50})	Doxorubicin HCl 0.4 µg/mL (IC_{50})	[38]
Flaviphenalenone B (**46**)	α-Glucosidase inhibition	Colorimetrically/α-Glucosidase	94.95 µM (IC_{50})	Acarbose 685.36 µM (IC_{50})	[38]
Flaviphenalenone C (**47**)	α-Glucosidase inhibition	Colorimetrically/α-Glucosidase	78.96 µM (IC_{50})	Acarbose 685.36 µM (IC_{50})	[38]
	Cytotoxicity	MTT/A549	28.5 µg/mL (IC_{50})	Doxorubicin HCl 0.2 µg/mL (IC_{50})	[38]
		MTT/MCF-7	50.0 µg/mL (IC_{50})	Doxorubicin HCl 0.4 µg/mL (IC_{50})	[38]
Auxarthrone A (**49**)	Antifungal	Serial dilution/*C. neoformans*	3.2 µg/mL (MIC)	Amphotericin B 0.8 µg/mL (MIC)	[39]
		Serial dilution/*C. albicans*	3.2 µg/mL (MIC)	Amphotericin B 0.8 µg/mL (MIC)	[39]
Auxarthrone B (**50**)	Antifungal	Serial dilution/*C. neoformans*	12.8 µg/mL (MIC)	Amphotericin B 0.8 µg/mL (MIC)	[39]
		Serial dilution/*C. albicans*	25.6 µg/mL (MIC)	Amphotericin B 0.8 µg/mL (MIC)	[39]
Auxarthrone D (**51**)	Antifungal	Serial dilution/*C. neoformans*	6.4 µg/mL (MIC)	Amphotericin B 0.8 µg/mL (MIC)	[39]
		Serial dilution/*C. albicans*	6.4 µg/mL (MIC)	Amphotericin B 0.8 µg/mL (MIC)	[39]
Auxarthrone C (**52**)	Antifungal	Serial dilution/*C. neoformans*	25.6 µg/mL (MIC)	Amphotericin B 0.8 µg/mL (MIC)	[39]

Compound Name	Biological Activity	Assay, Organism, or Cell Line	Biological Results	Positive Control	Ref.
		Serial dilution/*C. albicans*	51.2 µg/mL (MIC)	Amphotericin B 0.8 µg/mL (MIC)	[39]
FR-901235 (**54**)	Antifungal	Serial dilution/*C. neoformans*	51.2 µg/mL (MIC)	Amphotericin B 0.8 µg/mL (MIC)	[39]
		Serial dilution/*C. albicans*	51.2 µg/mL (MIC)	Amphotericin B 0.8 µg/mL (MIC)	[39]
Aspergillussanone D (**61**)	Antibacterial	Broth microdilution/*P. aeruginosa*	38.47 µg/mL (MIC_{50})	Streptomycin 0.34 µg/mL (MIC_{50})	[40]
		Broth microdilution/*S. aureus*	29.91 µg/mL (MIC_{50})	Penicillin 0.063 µg/mL (MIC_{50})	[40]
Aspergillussanone E (**62**)	Antibacterial	Broth microdilution/*E. coli*	7.83 µg/mL (MIC_{50})	Streptomycin 0.34 µg/mL (MIC_{50})	[40]
Aspergillussanone F (**63**)	Antibacterial	Broth microdilution/*P. aeruginosa*	26.56 µg/mL (MIC_{50})	Streptomycin 0.34 µg/mL (MIC_{50})	[40]
		Broth microdilution/*E. coli*	3.93 µg/mL (MIC_{50})	Streptomycin 0.25 µg/mL (MIC_{50})	[40]
		Broth microdilution/*S. aureus*	16.48 µg/mL (MIC_{50})	Penicillin 0.063 µg/mL (MIC_{50})	[40]
Aspergillussanone G (**64**)	Antibacterial	Broth microdilution/*P. aeruginosa*	24.46 µg/mL (MIC_{50})	Streptomycin 0.34 µg/mL (MIC_{50})	[40]
		Broth microdilution/*S. aureus*	34.66 µg/mL (MIC_{50})	Penicillin 0.063 µg/mL (MIC_{50})	[40]
Aspergillussanone H (**65**)	Antibacterial	Broth microdilution/*P. aeruginosa*	8.59 µg/mL (MIC_{50})	Streptomycin 0.34 µg/mL (MIC_{50})	[40]
		Broth microdilution/*E. coli*	5.87 µg/mL	Streptomycin 0.25 µg/mL	[40]

Compound Name	Biological Activity	Assay, Organism, or Cell Line	Biological Results	Positive Control	Ref.
			(MIC_{50})	(MIC_{50})	
Aspergillussanone I (**66**)	Antibacterial	Broth microdilution/*P. aeruginosa*	12.00 µg/mL (MIC_{50})	Streptomycin 0.34 µg/mL (MIC_{50})	[40]
Aspergillussanone J (**67**)	Antibacterial	Broth microdilution/*P. aeruginosa*	28.50 µg/mL (MIC_{50})	Streptomycin 0.34 µg/mL (MIC_{50})	[40]
		Broth microdilution/*E. coli*	5.34 µg/mL (MIC_{50})	Streptomycin 0.25 µg/mL (MIC_{50})	[40]
		Broth microdilution/*S. aureus*	29.87 µg/mL (MIC_{50})	Penicillin 0.063 µg/mL (MIC_{50})	[40]
Aspergillussanone K (**68**)	Antibacterial	Broth microdilution/*P. aeruginosa*	6.55 µg/mL (MIC_{50})	Streptomycin 0.34 µg/mL (MIC_{50})	[40]
		Broth microdilution/*S. aureus*	21.02 µg/mL (MIC_{50})	Penicillin 0.063 µg/mL (MIC_{50})	[40]
Aspergillussanone L (**69**)	Antibacterial	Broth microdilution/*P. aeruginosa*	1.87 µg/mL (MIC_{50})	Streptomycin 0.34 µg/mL (MIC_{50})	[40]
		Broth microdilution/*S. aureus*	2.77 µg/mL (MIC_{50})	Penicillin 0.063 µg/mL (MIC_{50})	[40]
		Broth microdilution/*B. subtilis*	4.80 µg/mL (MIC_{50})	Penicillin 0.063 µg/mL (MIC_{50})	[40]
(*S*)-2-((*S*,2*E*,6*E*,10*Z*)-14,15-Dihydroxy-11-(hydroxymethyl)-3,7,15-trimethylhexadeca-2,6,10-trien-1-yl)-2,4,6,9-tetrahydroxy-5,7-dimethyl-1*H*-phenalene-1,3(2*H*)-dione (**70**)	Antibacterial	Broth microdilution/*P. aeruginosa*	19.07 µg/mL (MIC_{50})	Streptomycin 0.34 µg/mL (MIC_{50})	[40]
		Broth microdilution/*E. coli*	1.88 µg/mL (MIC_{50})	Streptomycin 0.25 µg/mL (MIC_{50})	[40]

Compound Name	Biological Activity	Assay, Organism, or Cell Line	Biological Results	Positive Control	Ref.
Asperphenalenone A (**71**)	Anti-HIV-1	Luciferase assay/SupT1 cells	4.2 μM (IC_{50})	Lamivudine 0.1 μM (IC_{50}) Efavirenz 0.0004 μM (IC_{50})	[41]
Asperphenalenone B (**72**)	Anti-HIV-1	Luciferase assay/SupT1 cells	32.6 μM (IC_{50})	Lamivudine 0.1 μM (IC_{50}) Efavirenz 0.0004 μM (IC_{50})	[41]
Asperphenalenone D (**74**)	Anti-HIV-1	Luciferase assay/SupT1 cells	2.4 μM (IC_{50})	Lamivudine 0.1 μM (IC_{50}) Efavirenz 0.0004 μM (IC_{50})	[41]
	Anti-HIV-1	Luciferase assay/SupT1 cells	22.1 μM (IC_{50})	Lamivudine 0.1 μM (IC_{50}) Efavirenz 0.0004 μM (IC_{50})	[41]
Peniciphenalenin G (**83**)	Antimicrobial	Agar dilution/*B. cereus*	25.0 μM (MIC)	Ciprofloxacin 0.39 μM (MIC)	[35]
		Agar dilution/*Proteus* species	50.0 μM (MIC)	Ciprofloxacin 0.78 μM (MIC)	[35]
		Agar dilution/*M. Phlei*	50.0 μM (MIC)	Ciprofloxacin 0.39 μM (MIC)	[35]
		Agar dilution/*B. subtilis*	25.0 μM (MIC)	Ciprofloxacin 0.39 μM (MIC)	[35]
		Agar dilution/*V. Parahemolyticus*	50.0 μM (MIC)	Ciprofloxacin 0.39 μM (MIC)	[35]
		Agar dilution/MRCNS	25.0 μM (MIC)	Ciprofloxacin 25.0 μM (MIC)	[35]
		Agar dilution/MRSA	12.5 μM (MIC)	Ciprofloxacin > 50 μM (MIC)	[35]
Coniosclerodione (**85**)	Antimicrobial	Agar dilution/*B. cereus*	25.0 μM (MIC)	Ciprofloxacin 0.39 μM (MIC)	[35]
		Agar dilution/*Proteus* sp.	25.0 μM (MIC)	Ciprofloxacin 0.78 μM (MIC)	[35]
		Agar dilution/*M. Phlei*	25.0 μM (MIC)	Ciprofloxacin 0.39 μM (MIC)	[35]

Compound Name	Biological Activity	Assay, Organism, or Cell Line	Biological Results	Positive Control	Ref.
		Agar dilution/*B. subtilis*	12.5 μM (MIC)	Ciprofloxacin 0.39 μM (MIC)	[35]
		Agar dilution/*V. parahemolyticus*	12.5 μM (MIC)	Ciprofloxacin 0.39 μM (MIC)	[35]
		Agar dilution/MRCNS	12.5 μM (MIC)	Ciprofloxacin 25.0 μM (MIC)	[35]
		Agar dilution/MRSA	6.25 μM (MIC)	Ciprofloxacin > 50 μM (MIC)	[35]
Trypethelonamide A (**86**)	Cytotoxicity	CCK8/RKO	63.6 μM (IC_{50})	Taxol 0.05 μM (IC_{50})	[42]
5′-Hydroxytrypethelone (**87**)	Cytotoxicity	CCK8/RKO	22.6 μM (IC_{50})	Taxol 0.05 μM (IC_{50})	[42]
(+)-8-Hydroxy-7-methoxytrypethelone (**88**)	Cytotoxicity	CCK8/RKO	113.5 μM (IC_{50})	Taxol 0.05 μM (IC_{50})	[42]
		CCK8/HepG2	183.2 μM (IC_{50})	Taxol 1.0 μM (IC_{50})	[42]
(+)-Trypethelone (**89**)	Cytotoxicity	CCK8/RKO	49.3 μM (IC_{50})	Taxol 0.05 μM (IC_{50})	[42]
(−)-Trypethelone (**90**)	Cytotoxicity	CCK8/RKO	30.3 μM (IC_{50})	Taxol 0.05 μM (IC_{50})	[42]
O-Desmethylfunalenone (**100**)	Antibacterial	REMA/*B. subtilis*	265 μM (IC_{50})	Clotrimazole 0.4 μM (IC_{50})	[43]
	Cytotoxicity	Resazurin microplate/NS-1	70 μM (IC_{50})	5-Fluorouracil 4.6 μM (IC_{50})	[43]
Funalenone (**101**)	*h*PTP1B$_{1-400}$ inhibition	Photocolorimetric/*h*PTP1B$_{1-400}$	6.1 μM (IC_{50})	Ursolic acid 4.3 μM (IC_{50})	[44]
Hispidulone B (**103**)	Cytotoxicity	MTT/A-549	2.71 μM (IC_{50})	*cis*-Platinum 8.73 μM (IC_{50})	[45]
		MTT/Huh7	22.93 μM (IC_{50})	*cis*-Platinum 5.89 μM (IC_{50})	[45]

Compound Name	Biological Activity	Assay, Organism, or Cell Line	Biological Results	Positive Control	Ref.
		MTT/HeLa	23.94 μM (IC_{50})	*cis*-Platinum 14.68 μM (IC_{50})	[45]
Aceneoherqueinone A (**104**)	Angiotensin-I-converting enzyme inhibition	Spectrophotometric/Hippuryl-L-histidyl-L-leucine	3.10 μM (IC_{50})	Captopril 9.23 nM (IC_{50})	[46]
Aceneoherqueinone B (**105**)	Angiotensin-I-converting enzyme inhibition	Spectrophotometric/Hippuryl-L-histidyl-L-leucine	11.28 μM (IC_{50})	Captopril 9.23 nM (IC_{50})	[46]
Erabulenol B (**117**)	Indoleamine dioxygenase 1 inhibition	ELISA/Indoleamine 2,3-dioxygenase 1	13.69 μM (IC_{50})	Epacadostat 0.015 μM (IC_{50})	[47]
Erabulenol C (**118**)	Indoleamine dioxygenase 1 inhibition	ELISA/Indoleamine 2,3-dioxygenase 1	14.38 μM (IC_{50})	Epacadostat 0.015 μM (IC_{50})	[47]
Duclauxin (**120**)	Antitumor	ELISA/EGFR	0.95 μM (IC_{50})	Afatinib 0.0005 μM (IC_{50})	[48]
		ELISA/CDC25B	0.75 μM (IC_{50})	Na_3VO_4 0.52 μM (IC_{50})	[48]
	Cytotoxicity	Resazurin microplate/NS-1	140 μM (IC_{50})	5-Fluorouracil 4.6 μM (IC_{50})	[43]
	*h*PTP1B$_{1-400}$ inhibition	Photocolorimetric/*h*PTP1B$_{1-400}$	12.7 μM (IC_{50})	Ursolic acid 26.6 μM (IC_{50})	[49]
Talaromycesone A (**121**)	Antibacterial	REMA/*S. epidermidis*	3.70 μM (IC_{50})	Chloramphenicol 1.81 μM (IC_{50})	[50]
	Antibacterial	REMA/MRSA	5.48 μM (IC_{50})	Chloramphenicol 2.46 μM (IC_{50})	[50]
	AchE inhibition	Modified Ellman's enzyme/Immunosorbent assay	7.49 μM (IC_{50})	Huperzine 11.60 μM (IC_{50})	[50]
Talaromycesone B (**122**)	Antibacterial	REMA/*S. epidermidis*	17.36 μM (IC_{50})	Chloramphenicol 1.81 μM (IC_{50})	[50]
		REMA/MRSA	19.50 μM	Chloramphenicol 2.46 μM (IC_{50})	[50]

[30]

[32]

eparatory onone A2 up at C-8 ethyl-1H- eagent in ed potent .10 mM), ber of OH

Compound Name	Biological Activity	Assay, Organism, or Cell Line	Biological Results	Positive Control	Ref.
			(IC_{50})		
	*h*PTP1B$_{1-400}$ inhibition	Photocolorimetric/*h*PTP1B$_{1-400}$	82.1 µM (IC_{50})	Ursolic acid 26.6 µM (IC_{50})	[49]
Bacillisporin A (**123**)	Antibacterial	Microtiter plate/*S. aureus*	5.2 µg/mL (MIC)	Tetracycline 0.05 µg/mL (MIC)	[51]
		Microtiter plate/*S. hemolyticus*	9.5 µg/mL (MIC)	Tetracycline 29.2 µg/mL (MIC)	[51]
		Microtiter plate/*E. faecalis*	2.4 µg/mL (MIC)	Tetracycline 0.4 µg/mL (MIC)	[51]
9a-*Epi*-bacillisporin E (**124**)	Antibacterial	Microtiter plate/*S. aureus*	29.3 µg/mL (MIC)	Tetracycline 0.05 µg/mL (MIC)	[51]
Bacillisporin F (**125**)	Antibacterial	Microtiter plate/*S. aureus*	15.6 µg/mL (MIC)	Tetracycline 0.05 µg/mL (MIC)	[51]
	Antitumor	ELISA/EGFR	4.41 µM (IC_{50})	Afatinib 0.0005 µM (IC_{50})	[48]
		ELISA/CDC25B	0.40 µM (IC_{50})	Na_3VO_4 0.52 µM (IC_{50})	[48]
	Antitumor	ELISA/EGFR	4.41 µM (IC_{50})	Afatinib 0.0005 µM (IC_{50})	[48]
		ELISA/CDC25B	0.40 µM (IC_{50})	Na_3VO_4 0.52 µM (IC_{50})	[48]
Bacillisporin G (**127**)	*h*PTP1B$_{1-400}$ inhibition	Photocolorimetric/*h*PTP1B$_{1-400}$	13.5 µM (IC_{50})	Ursolic acid 26.6 µM (IC_{50})	[49]
Bacillisporin H (**128**)	Cytotoxicity	MTT/HeLa	49.5 µM (IC_{50})	Cisplatin 10.6 µM (IC_{50})	[51]
	Antibacterial	Microtiter plate/*S. aureus*	5.0 µg/mL (MIC)	Tetracycline 0.05 µg/mL (MIC)	[51]
		Microtiter plate/*S. hemolyticus*	20.4 µg/mL (MIC)	Tetracycline 29.2 µg/mL (MIC)	[51]

act. They
figuration
t, and the
ted weak
icroplate
ested cell
arum and
lioisotope

e (**8**), 12-
, and 4-
e-derived

Penicillium sp. (**Figure 2**). The new metabolites' configuration was assigned, based on specific rotations and chemical modifications. Compound **17** exhibited moderate anti-inflammatory activity (IC_{50} 3.2 µM) towards mouse macrophage RAW 264.7 cells, compared to AMT (IC_{50} 0.2 µM) in the nitric oxide synthase assay. In addition, **27**

Compound Name	Biological Activity	Assay, Organism, or Cell Line	Biological Results	Positive Control	Ref.
Verruculosin A (**129**)	Antitumor	ELISA/EGFR	0.92 μM (IC_{50})	Afatinib 0.0005 μM (IC_{50})	[48]
	Antitumor	ELISA/CDC25B	0.38 μM (IC_{50})	Na_3VO_4 0.52 μM (IC_{50})	[48]
Verruculosin B (**130**)	Antitumor	ELISA/EGFR	1.22 μM (IC_{50})	Afatinib 0.0005 μM (IC_{50})	[48]
Xenoclauxin (**131**)	Antitumor	ELISA/EGFR	0.24 μM (IC_{50})	Afatinib 0.0005 μM (IC_{50})	[48]
		ELISA/CDC25B	0.26 μM (IC_{50})	Na_3VO_4 0.52 μM (IC_{50})	[48]
	*h*PTP1B$_{1-400}$ inhibition	Photocolorimetric/*h*PTP1B$_{1-400}$	21.8 μM (IC_{50})	Ursolic acid 26.6 μM (IC_{50})	[49]

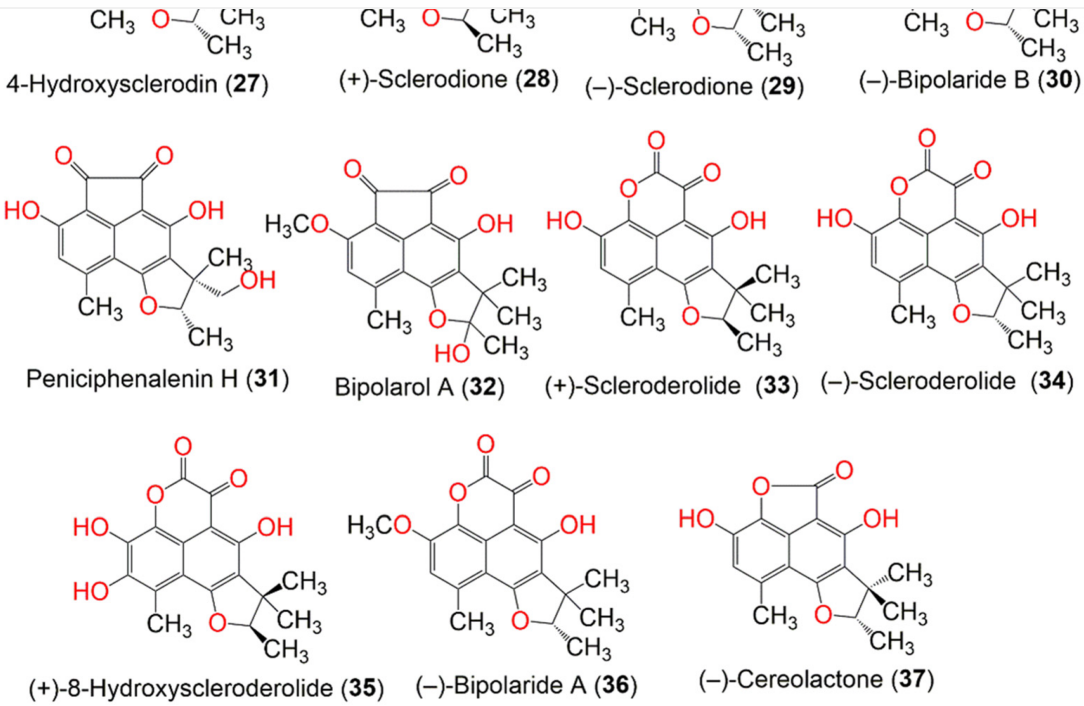

Figure 2. The structures of compounds **11–22**.

Lee et al. purified **18** from a culture of *Penicillium herquei* FT729, derived from Hawaiian volcanic soil by LC-MS-guided chemical analysis. It was identified by spectroscopic analysis, optical rotation, and LC-MS analysis. The pretreatment of T cells with **18** remarkably reduced IL-2 production and the expression of surface molecules, including CD-25 and -69, and activated T cell proliferation after TCR-mediated stimulation, as well as abrogating the NF-κB and MAPK pathways. Therefore, it effectively down-regulated T cell activity via the MAPK pathway, which indicated its immunosuppressive potential [53]. Furthermore, *P. herquei* PSURSPG93, obtained from soil, produced a new derivative, peniciherqueinone (**7**), along with the formerly separated derivatives: herqueinone (**9**), deoxyherqueinone (**14**), the acetone adduct of atrovenetinone (**18**) (as a mixture of epimers), sclerodin (**20**), and

(−)-7,8-dihydro-3,6-dihydroxy-1,7,7,8-tetramethyl-5H-furo-[2′,3′,:5,6]naphtho[1,8-*bc*]furan-5-one (**37**). Compound **7** was structurally similar to **9**, except for the disappearance of one olefinic proton signal. Its *R*-configuration at C-4 was determined by an anisotropic effect and CD spectroscopy, which was opposite to **9**. Compounds **9**, **14**, and **20** had no cytotoxic effect toward MCF-7, KB, and noncancerous Vero cell lines. In addition, only **9** exhibited mild antioxidant potential, where it inhibited $OH^{\bullet}$, $DPPH^{\bullet}$, and $O_2^{\bullet-}$ (IC_{50} 0.48, 6.34, and 4.11 mM, respectively) in the hydroxyl radical, DPPH, and superoxide radical scavenging assays, respectively, in comparison with tannic acid ($OH^{\bullet}$, IC_{50} 0.26), butylated hydroxytoluene ($DPPH^{\bullet}$, IC_{50} 0.11), and trolox ($O_2^{\bullet-}$, IC_{50} 0.96 mM) [33].

Intaraudom et al. purified the new derivatives, **25**, **26**, **30**, **32**, **36**, and **39–42**, together with **22** and **34**, from the broth EtOAc extract of the marine-derived *Lophiostoma bipolare* BCC25910 (**Figure 3**). Their structures were assigned via spectroscopic analysis, whereas the C-2′, S-configuration was determined based on X-ray analysis, a chemical reaction, and a specific optical rotation negative sign. They showed no antimalarial activity toward the *P. falciparum* K-1 strain and no antifungal activity toward *C. albicans*. On the other hand, **25**, **26**, **36**, **39**, and **40** showed moderate antibacterial potential toward *B. cereus* (MICs 12.5 µg/mL). However, other compounds were inactive against *B. cereus* (concentration 25 µg/mL). Additionally, they exhibited weak cytotoxicity toward KB, MCF-7, NCI-H187, and Vero cells [36].

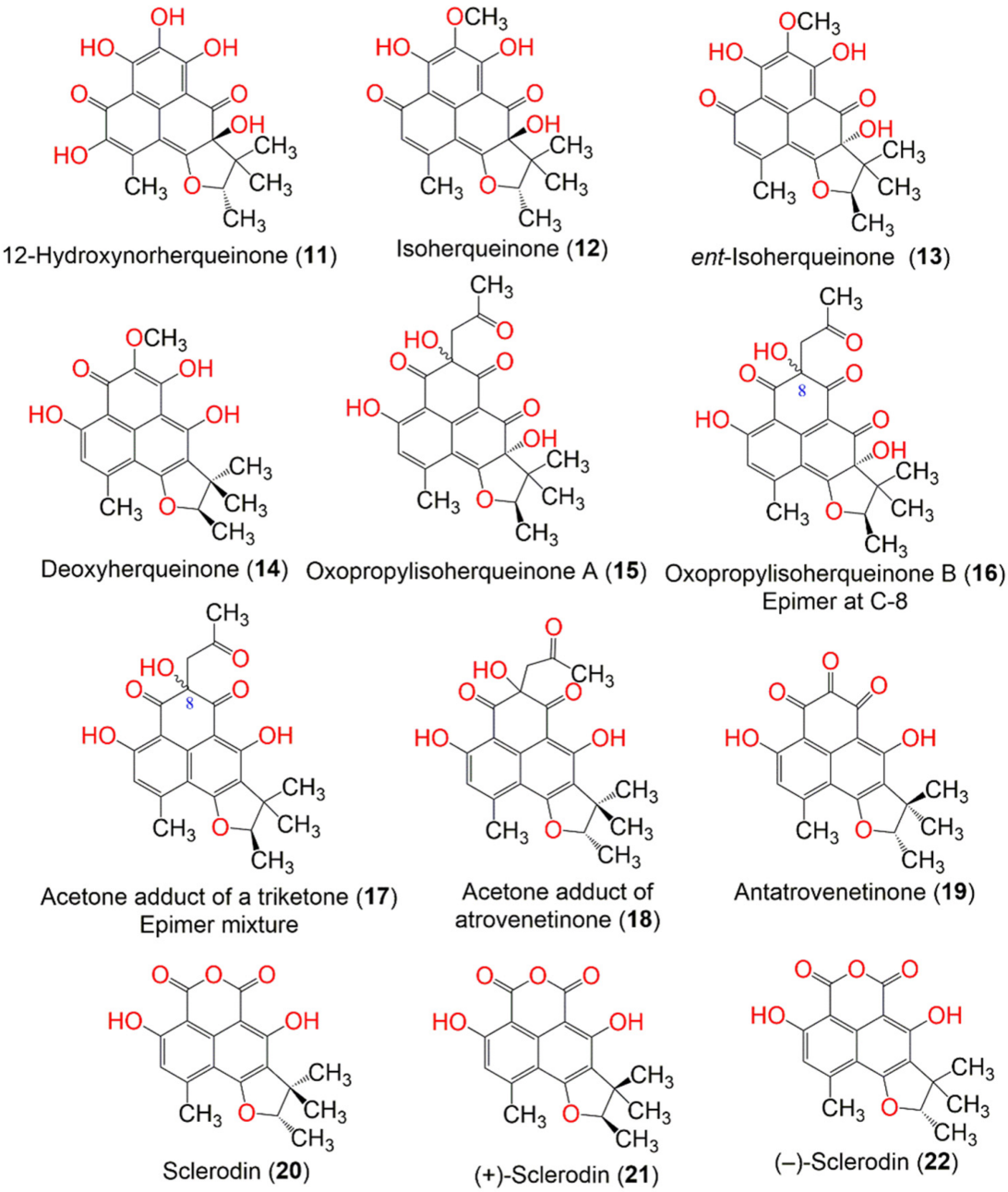

Figure 3. The structures of compounds **23–37**.

Macabeo et al. purified **29**, **34**, and **90** from a culture of *Pseudolophiostoma* sp. MFLUCC-17-2081 obtained from a dried branch of *Clematis fulvicoma*. Compounds **29** and **34** conferred more potent α-glucosidase inhibition (IC_{50} 48.7 and 120 μM, respectively) than N-deoxynojirimycin (IC_{50} 130.5 μM). They also potently inhibited the hydrolysis of *p*-nitro-phenylbutyrate, using porcine lipase. Interestingly, **29** and **34** showed stronger inhibitory potential (IC_{50}s 1.0 and 3.4 μM, respectively) than orlistat (IC_{50} 9.4 μM). The in silico techniques employed revealed that **29** and **34** exhibited strong binding affinities to porcine pancreatic lipase and α-glucosidase through π–π and H-bonding interactions, while **90** was weakly active (IC_{50} > 100 μM) toward both enzymes [37].

Zhang et al. purified new derivatives, flaviphenalenones A–C (**45**–**47**), from solid cultures of *Aspergillus flavipes* PJ03-11 (**Figure 4**). The 6*S* absolute configuration of **45** was determined by the computational ECD method.

Compound **47** was a positional isomer of **46**. They represented the first report of phenalenones with a directly connected C-10 isoprene unit, whereas **47** had a keto-lactone group at C-8. Compounds **46** and **47** possessed potent α-glucosidase inhibitory potential (IC_{50}s 94.95 and 78.96 μM, respectively) than acarbose (IC_{50} 685.36 μM). On the other hand, **45** displayed significant cytotoxic capacities toward MCF-7 and A549 (IC_{50} 10.0 and 6.6 μg/mL, respectively) compared to doxorubicin (IC_{50} 0.4 and 0.2 μg/mL, respectively), while **47** showed moderate cytotoxicity toward A549 (IC_{50} 28.5 μg/mL) [38].

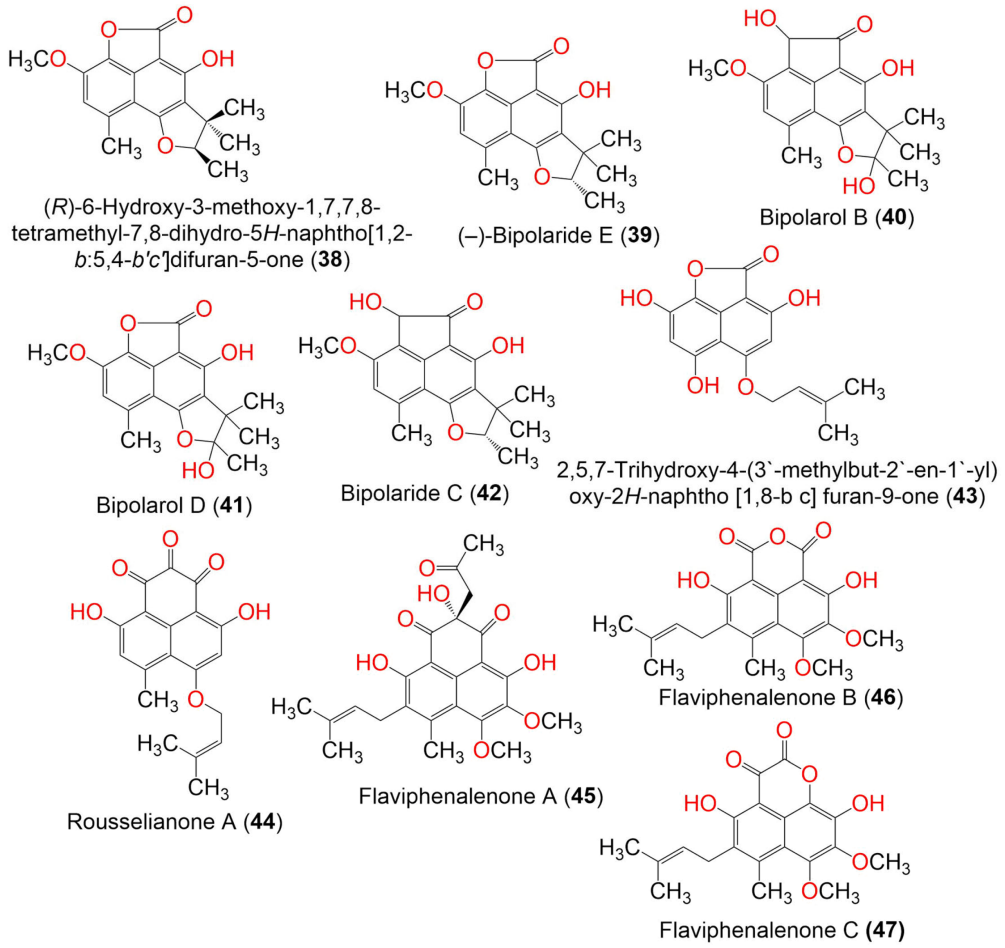

Figure 4. The structures of compounds **38**–**47**.

Auxarthrones A–E (**49**–**53**) and FR-901235 (**54**) were obtained from the culture of the coprophilous fungus *Auxarthron pseudauxarthron* TTI-0363 (**Figure 5**). Compounds **52** and **53** possessed an unusual 7a,8-dihydrocyclopenta[*a*]phenalene-7,9-dione ring system. Compound **49** was separated into a mixture of racemic diastereomers; their structures were confirmed by X-ray crystallography. Compounds **49** and **51** showed moderate antifungal potential toward *C. albicans* and *C. neoformans* (MICs 6.4 and 3.2 μg/mL, respectively), compared to amphotericin B (MIC 0.8 μg/mL). The other phenalenones were weakly active (MIC ranging from 6.4 to 51.2 μg/mL). On the other hand, they showed no significant cytotoxic effects against MDA-MB-451 and MDA-MB-231 [39].

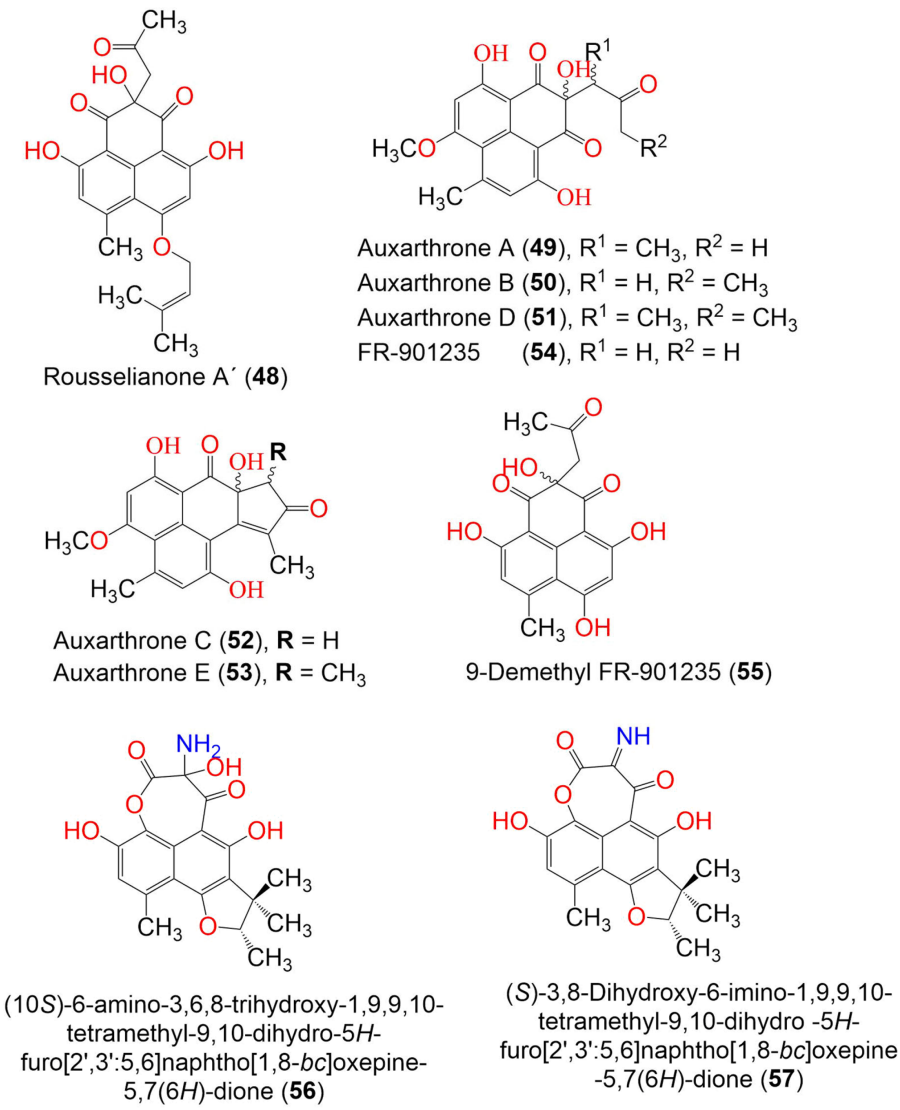

Figure 5. The structures of compounds **48–57**.

Compound **56** obtained from the marine-derived endophytic fungus, *Coniothyrium cereale,* harboring the Baltic Sea algae *Enteromorpha* sp., which had unprecedented imine functionality between two carbonyls to produce an oxepane-imine-dione ring. It exhibited a moderate cytotoxic potential toward the SKM1, U266, and K562 cancer cell lines (IC_{50}s 75.0, 45.0, and 8.5 µM, respectively) in the MTT assay [54]. The new phenalenone derivatives, aspergillussanones C–L (**60**–**69**), along with the known analog **70**, were isolated from the solid culture of *Aspergillus* sp. that was associated with *Pinellia ternate* (**Figure 6** and **Figure 7**).

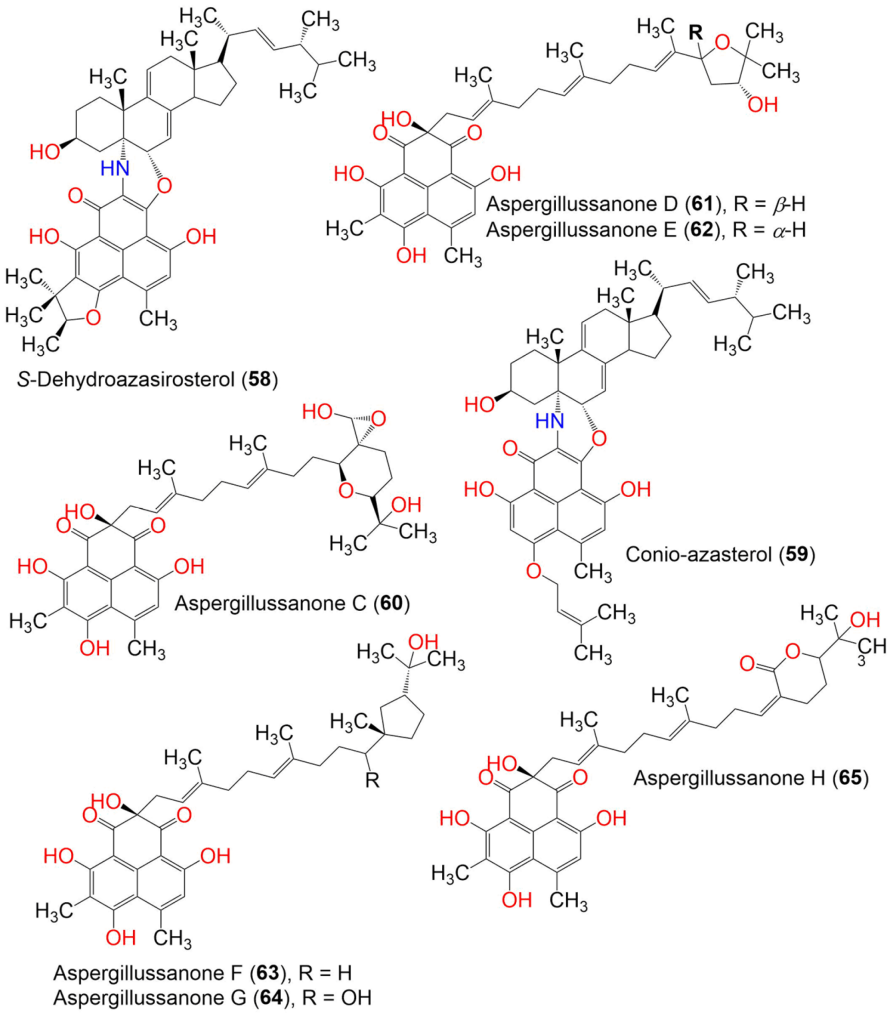

Figure 6. The structures of compounds **58–65**.

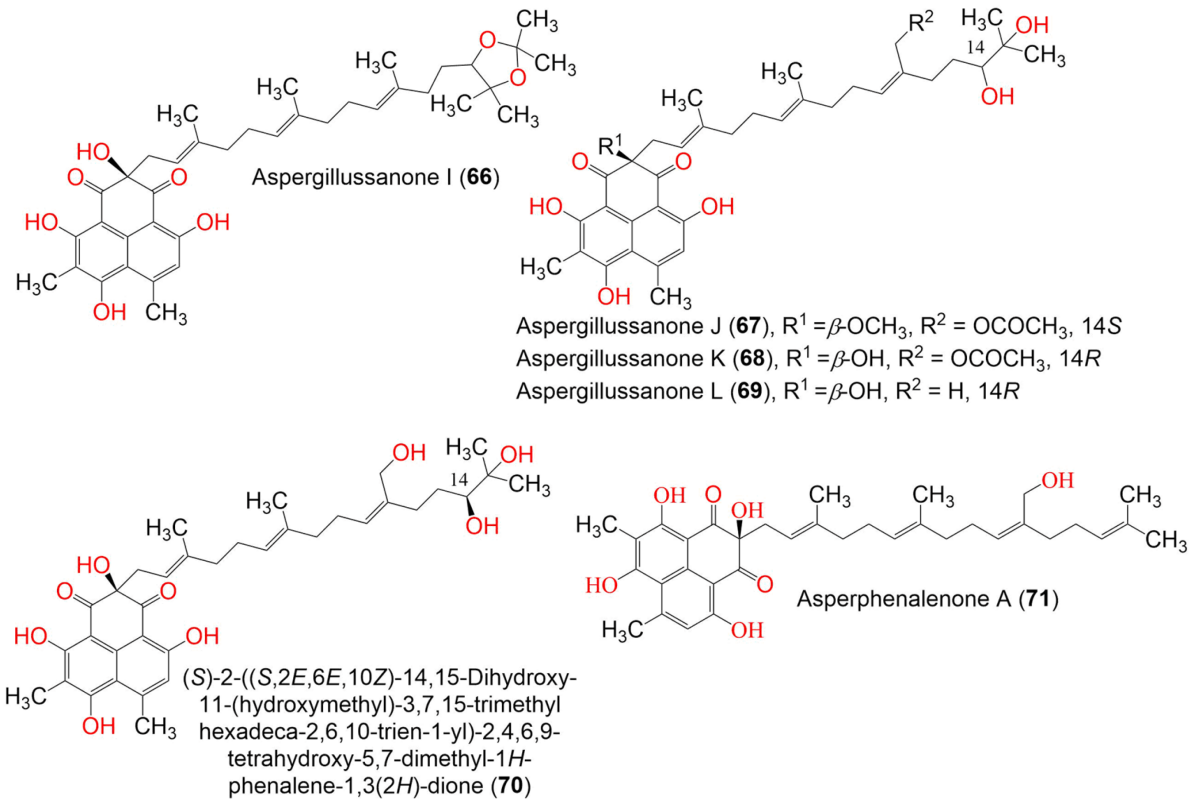

Figure 7. The structures of compounds **66–71**.

Compounds **60**–**69** are unusual acyclic diterpenoid adducts that are partly epoxidized and variously oxidized to produce diverse heterocyclic analogs. Their structures and absolute configurations were established by spectroscopic, ECD, and $Mo_2(OCOCH_3)_4$-induced ECD analyses. Their antibacterial effectiveness toward *Pseudomonas aeruginosa, Escherichia coli, Staphylococcus aureus,* and *Bacillus subtilis* was evaluated using the broth micro-dilution method. Compound **69** exhibited the most potent antibacterial potential against *B. subtilis, S. aureus,* and *P. aeruginosa* (MIC 4.80, 2.77, and 1.87 µg/mL, respectively), compared to streptomycin (MIC 0.34 µg/mL for *P. aeruginosa*) and penicillin (MIC 0.063 and 0.13 µg/mL for *S. aureus* and *B. subtilis,* respectively). Compounds **65**–**67** had potential versus *P. aeruginosa* (MIC_{50}s 6.55–12.00 µg/mL). Meanwhile, **62**, **63**, **65**, and **67** showed significant activity toward *E. coli* (MIC 3.93–7.83 µg/mL) [40].

Aspergillus sp. CPCC 400735, which is associated with *Kadsura longipedunculata,* was found to biosynthesize the structurally unusual phenalenones, asperphenalenones A–E (**71**–**75**), these having a linear diterpene moiety that is connected to the phenalenone skeleton through a C-C bond (**Figure 8**). Their structures were established from extensive NMR spectroscopic analyses, while the absolute configuration was determined based on the CD spectra. Compounds **71** and **74** exhibited anti-HIV activity (IC_{50} 4.5 and 2.4 µM, respectively), in comparison to lamivudine (IC_{50} 0.1 µM) and efavirenz (IC_{50} 0.0004 µM), using SupT1 cells in the luciferase assay system, while **72** and **75** exhibited weak activity (IC_{50} 32.6 and 22.1 µM, respectively) [41].

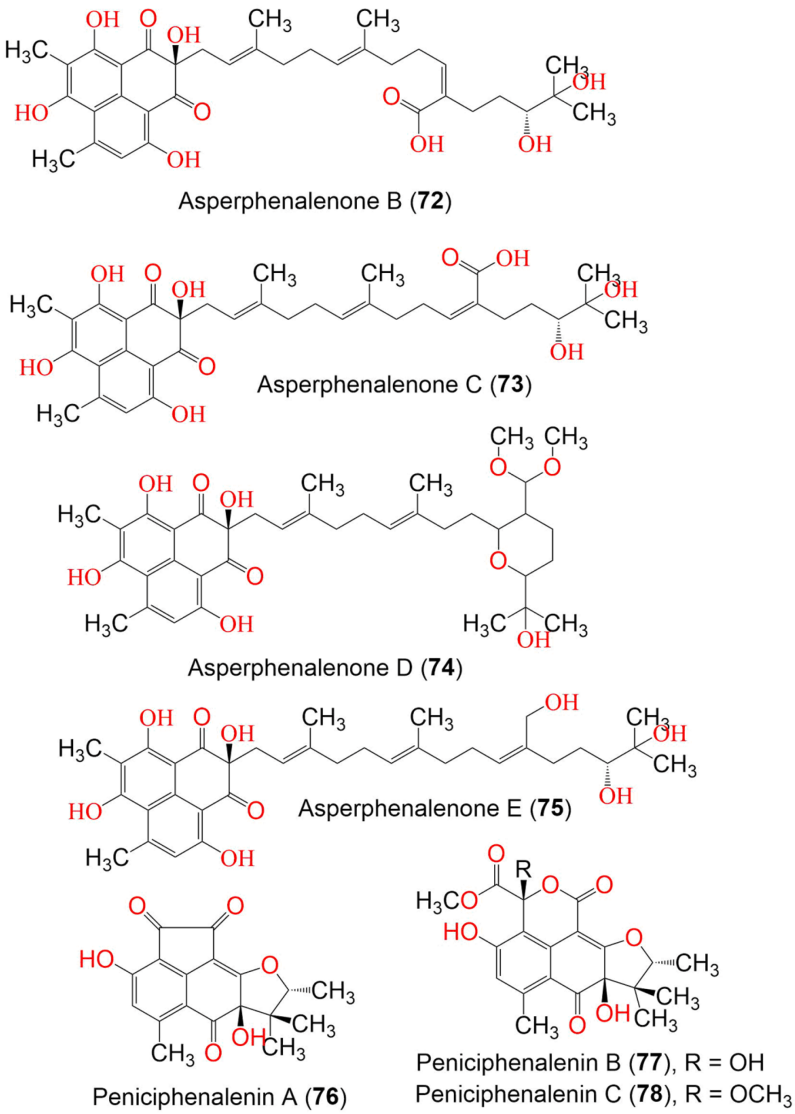

Figure 8. The structures of compounds **72**–**78**.

The new derivatives, peniciphenalenins A–F (**76**–**81**), along with the formerly reported **21**, **28**, and **33**, were obtained from *Penicillium* sp. ZZ901 culture, using ODS and HPLC (**Figure 9**). Their structures were determined by extensive spectroscopic analysis, ECD calculation, optical rotation, and single X-ray diffraction. The analyses identified a phenalenone skeleton, fused to a trimethyl-furan ring. Compounds **28** and **33** showed antimicrobial activity toward MRSA and *E. coli* (MICs 23–35 µg/mL for **28** and 7.0–9.0 µg/mL for **33**). On the other hand, **21**, **28**, and **33** showed weak antiproliferative activity against the glioma cells (IC_{50} 23.24–6.93 µM), compared to doxorubicin (IC_{50} 1.2 and 0.47 µM, respectively) [34].

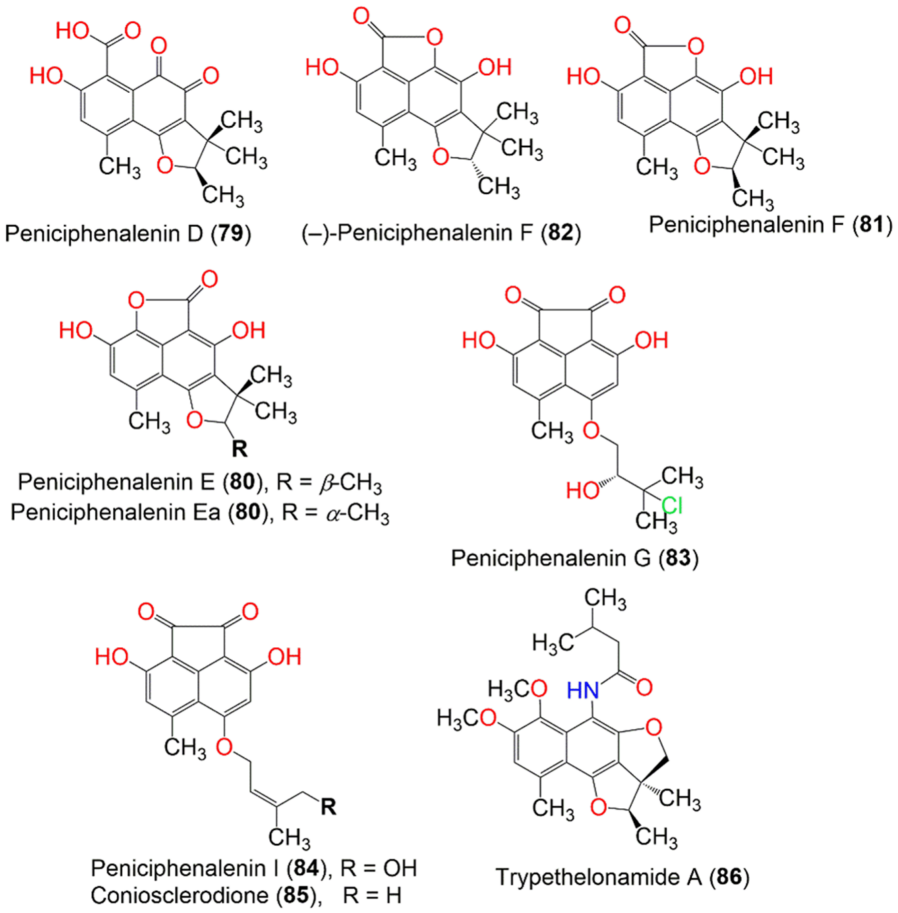

Figure 9. The structures of compounds **73**–**86**.

Han et al. separated three new red-colored phenalenone derivatives, peniciphenalenins G–I (**83**, **31**, and **84**), along with coniosclerodione (**85**) and (−) sclerodinol (**24**) from the marine sediment-derived fungus, *Pleosporales* sp. HDN1811400, using UV-HPLC guided investigation. Their absolute configurations were determined by detailed spectroscopic and ECD analyses, in addition to the chemical method. Compound **83** was the first example of a chlorinated phenalenone derivative. Compounds **24, 31**, **83**, and **85** showed antimicrobial potential versus *B. cereus, Proteus* sp., *M. phlei, B. subtilis, V. parahemolyticus, E. tarda,* MRCNS, and MRSA (MICs 6.25–50.0 µM). Compound **85** (MIC 6.25 µM) was more active than compound **84**, indicating that 19-OH reduced the activity. Notably, compounds **24**, **31**, **83**, and **85** showed better inhibitory potential toward MRCNS and MRSA than that of ciprofloxacin, indicating their potential regarding drug-resistant strains [35].

Basnet et al. reported the isolation of a new yellow compound, trypethelonamide A (**86**), and a new dark violet-red compound, 5′,-hydroxytrypethelone (**87**), along with a dark violet-red metabolites (+)-8-hydroxy-7-methoxytrypethelone (**88**), (+)-trypethelone (**89**), and (−)-trypethelone (**90**) from the cultured lichenized fungus *Trypethelium eluteriae* by using Sephadex LH-20, ODS, SiO_2, and HPLC. They were fully characterized via spectroscopic and ECD spectral analyses (**Figure 10**). They showed moderate to weak cytotoxicity versus the RKO cell line (IC_{50} ranged from 22.6 to 113.5 µM), compared to taxol (IC_{50} 0.05 µM) in the CCK8 assay, while they had no antioxidant potential in the DPPH assay (concentration 200 µM) [42].

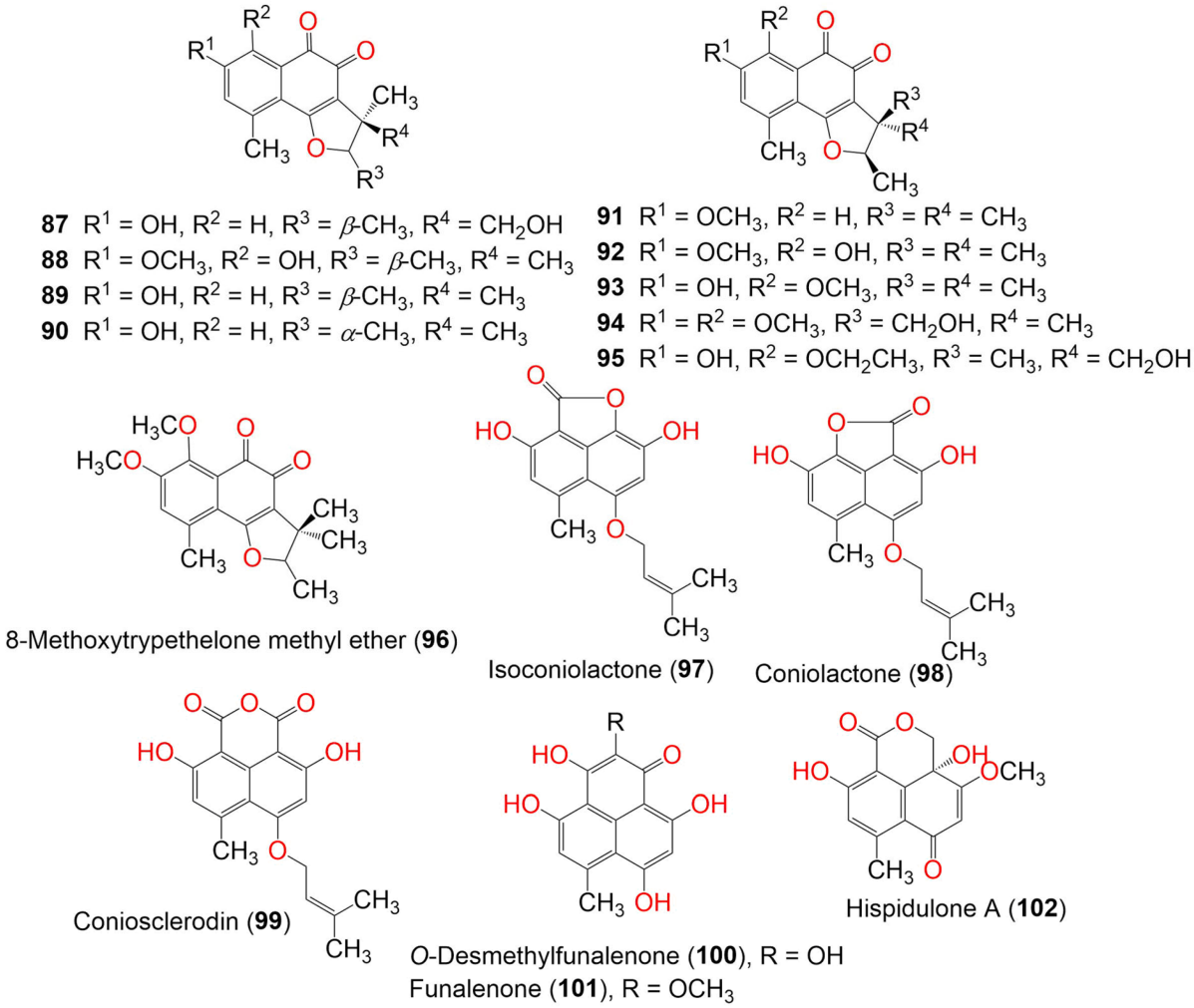

Figure 10. The structures of compounds **87**–**102**.

Two new metabolites, 8-methoxytrypethelone (**93**) and 5′-hydroxy-8-ethoxytrypethelone (**95**), along with compounds **20**, **38**, **89**, **91**, **92**, and **94** were separated from mycobiont culture of *Trypethelium eluteriae* by preparative TLC and column chromatography. They were fully characterized by using spectroscopic, ECD, and X-ray analyses. Compound **89** (MIC 12.5 µg/mL) showed potent antimycobacterial potential toward *M. tuberculosis,* followed by **38** and **94** (MIC 50.0 µg/mL). Moreover, **89** had moderate potential (MIC 25.0 µg/mL) toward *M. chitae, M. szulgai, M. phlei, M. flavescens, M. parafortuitum,* and *M. kansasii*. In addition, compounds **89** and **94** were active versus *S. aureus* (MIC 25 µg/mL) [55]. Funalenone (**101**) was also purified as a PTP inhibitor from a marine-derived fungal strain of *Aspergillus* sp. SF-5929 and was tested for its inhibitory potential on *h*PTP1B$_{1-400}$ in a photocolorimetric assay using the *h*PTP1B$_1$ enzyme. It exhibited powerful PTP1B inhibitory potential (IC$_{50}$ 6.1 µM), compared to ursolic acid (IC$_{50}$ 4.3 µM). It was found that **101** was a noncompetitive PTP1B inhibitor that targeted the active or allosteric site of the enzyme [44]. *Chaetosphaeronema hispidulum* yielded two new phenalenones, hispidulones A (**102**) and B (**103**), which were assigned by spectroscopic and ECD analyses (**Figure 11**).

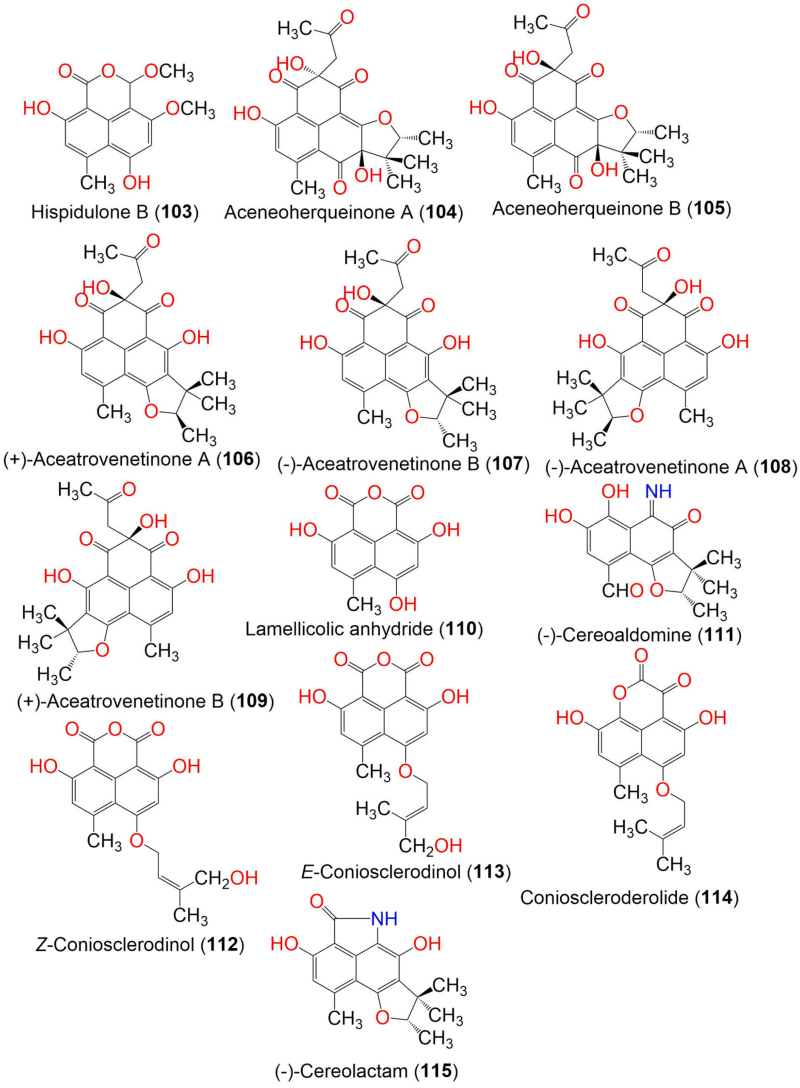

Figure 11. The structures of compounds **103**–**115**.

Compound **102** had a cyclohexa-2,5-dien-1-one moiety, whereas **103** possessed a hemiacetal OCH_3 group that was uncommon in phenalenone analogs. Compound **103** showed cytotoxic potential toward A-549, Huh7, and HeLa cells (IC_{50} 2.71, 22.93, and 23.94 μM, respectively), compared with *cis*-platinum (IC_{50} 8.73, 5.89, and 14.68 μM, respectively), whereas **102** did not show any effect in the MTT assay [45].

Aceneoherqueinones A (**104**) and B (**105**), (+)-aceatrovenetinone A (**106**), and (+)-aceatrovenetinone B (**109**), along with the known congeners, (+)-scleroderolide (**33**), (−)-scleroderolide (**34**), (−)-aceatrovenetinone B (**107**), and (−)-aceatrovenetinone A (**108**), were reported from the marine mangrove-derived fungus, *Penicillium herquei* MA-370. Among these, compounds **104** and **105** were rare phenalenones, having a cyclic ether unit between C-2′ and C-5 (**Figure 11**). Compounds **106**–**109** were unstable stereoisomers, possessing configurationally labile chiral centers that were characterized by HPLC-ECD analyses, assisted by TDDFT-ECD calculations. The absolute configuration of **104** was confirmed by X-ray, while those of **105**–**109** were established by ECD spectra TDDFT-ECD calculations. Compounds **104** and **105** displayed ACE (angiotensin-I-converting enzyme) inhibitory activity (IC_{50}s 3.10 and 11.28 μM, respectively), compared to captopril (IC_{50} 9.23 nM). The molecular docking study

revealed that compound **104** bound well with ACE via hydrogen interactions with the residues Gln618, Ala261, Asn624, and Trp621, while **105** interacted with the Tyr360 and Asp358 residues. This difference in interactions was likely caused by the C-8 epimerization of both compounds [46].

Penicillium herquei FT729, which is associated with Hawaiian volcanic soil, yielded herqueilenone A (**116**) and erabulenols B (**117**) and C (**118**) (**Figure 12**). Their structures were determined by spectroscopic analysis, ECD calculations, and GIAO (gauge-including atomic orbital) NMR chemical shifts. Compounds **117** and **118** exhibited significant IDO1 (indoleamine 2,3-dioxygenase 1) inhibitory activities (with IC_{50} values of 13.69 and 14.38 μM, respectively), compared to epacadostat (IC_{50} 0.015 μM). Therefore, they can be developed into cancer immunotherapeutics. Compounds **117** and **118** also exhibited a protective effect toward acetaldehyde-induced damage in PC-12 cells and significantly increased cell viability [47].

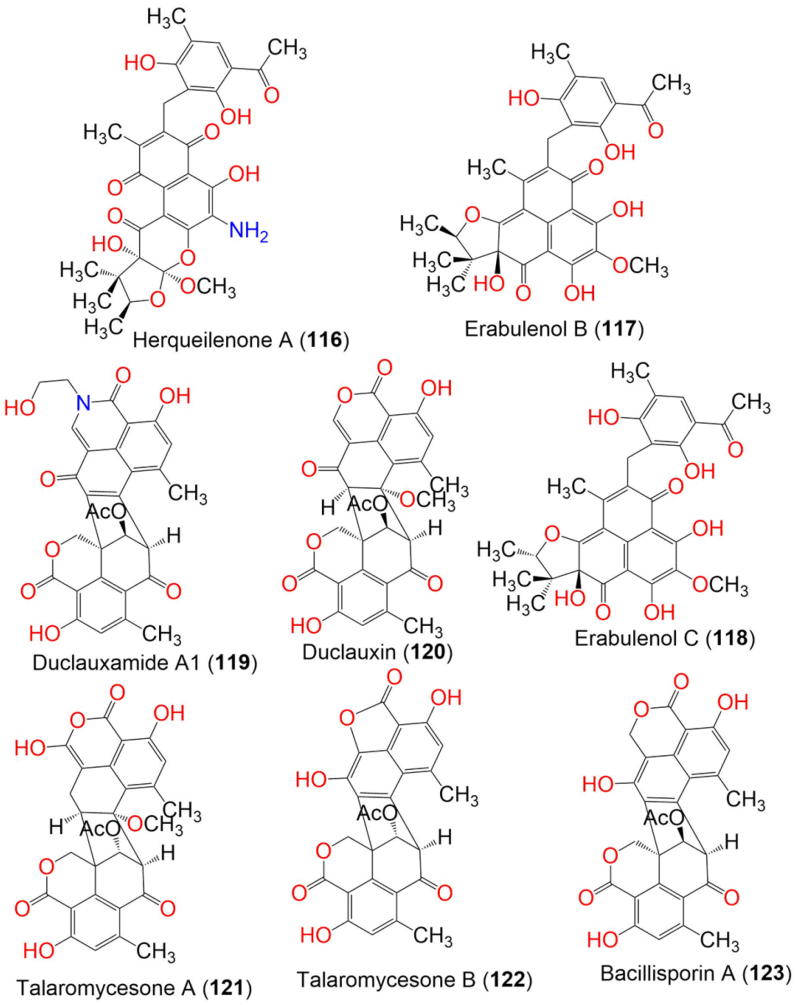

Figure 12. Structures of compounds **116**–**123**.

Duclauxamide A1 (**119**), a new polyketide heptacyclic-oligophenalenone dimer with an *N*-2-hydroxyethyl moiety, was isolated from *Penicillium manginii* YIM PH30375, which is associated with *Panax notoginseng*. It belongs to the 9′S-duclauxin epimers, based on spectroscopic data analysis, single-crystal X-ray diffraction, and the computational ^{13}C NMR-DFT method. It is structurally related to duclauxin (**120**), showing the replacement of the

O-atom with the *N*-containing chain, without modification, on the original carbon skeleton. It showed moderate cytotoxicity toward MCF-7, SMML-7721, A-549, HL-60, and SW480 (IC_{50} ranged from 11 to 32 μM), compared to cisplatin and paclitaxel [56]. Two new oxaphenalenone dimers, talaromycesones A (**121**) and B (**122**), were isolated from the marine fungus *Talaromyces* sp. LF458 culture broth and mycelia. Their relative configuration was determined by NOESY spectral data. Compound **116** was the first metabolite with a 1-nor oxaphenalenone dimer framework. They exhibited significant antibacterial potential toward *S. epidermidis* and *S. aureus* (IC_{50}s 3.70 and 5.48 μM, respectively, for **121**, and 17.36 and 19.50, respectively, for **122**), compared to chloramphenicol (IC_{50} 1.81 and 2.46 μM, respectively) in the resazurin microplate assay. They revealed no antifungal effectiveness toward *Trichophyton rubrum* and *C. albicans*. Moreover, **121** exhibited AchE (acetylcholinesterase) inhibition (IC_{50} 7.49 μM) that was more powerful than huperzine (IC_{50}, 11.60 μM) in the modified Ellman's enzyme/immunosorbent assay [50].

In the case of 9a-*epi*-bacillisporin E (**124**) and bacillisporins F–H (**125**, **127**, and **128**), new oligophenalenone dimers, along with bacillisporin A (**123**), were separated from a culture of *Talaromyces stipitatus* (**Figure 13**). Their absolute configurations and structures were determined based on spectroscopic analyses, ECD, and GIAO NMR shift calculation, followed by DP4 probability analysis. Only **128** was moderately active (IC_{50} 49.5 μM) toward the HeLa cell, compared to cisplatin (IC_{50} 10.6 μM). No effect was observed on the growth of *E. coli* (IC_{50} > 100 μg/mL) for all isolated compounds, while **123** displayed noticeable antibacterial potential versus *Staphylococcus hemolyticus, S. aureus* (ATCC 6538), and *Enterococcus faecalis* (MICs 9.5, 5.2, and 2.4 μg/mL, respectively), compared to tetracycline (MICs 29.2, 0.05, and 0.4 μg/mL, respectively). However, **128** had an observable effect on *S. aureus* (MIC 5.0 μg/mL) when using a microtiter plate assay [51].

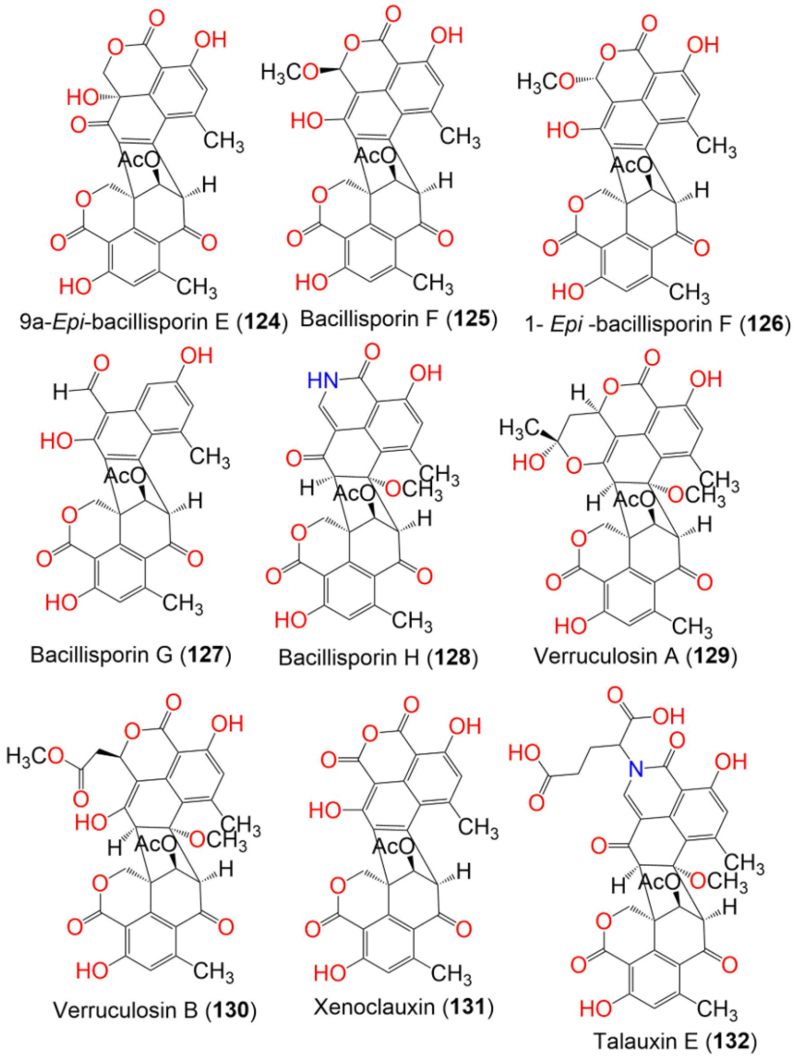

Figure 13. The structures of compounds **124**–**132**.

Talaromyces verruculosus yielded two new oligophenalenone dimers, verruculosins A (**129**) and B (**130**), and the related known analogs, duclauxin (**120**), bacillisporin F (**125**), and xenoclauxin (**131**) (**Figure 13**). Compound **129** was a novel oligophenalenone dimer with a unique octacyclic skeleton. Compounds **129** and **130** were fully characterized by spectroscopic, X-ray crystallography, and ECD analyses as well as, optical rotation and NMR calculations. Compounds **120**, **125**, **129**, and **131** exhibited potent CDC25B inhibitory activities (IC_{50} values of 0.75, 0.40, 0.38, and 0.26 μM, respectively), compared to Na_3VO_4 (IC_{50} 0.52 μM). In addition, **120** and **129**–**131** displayed moderate EGFRIC inhibitory activities (IC_{50} values from 0.24 to 1.22 μM) in comparison to afatinib (IC_{50} 0.0005 μM). The results revealed that oligophenalenone dimers could be used as CDC25B inhibitor candidates [48].

Duclauxin (**120**), talaromycesone B (**122**), bacillisporin G (**127**), and xenoclauxin (**131**) were isolated from anthill soil fungus *Talaromyces* sp. IQ-313. They were evaluated for PTP (protein tyrosine phosphatases) inhibitory potential. They inhibited *h*PTP1B$_{1-400}$ (IC_{50} values ranging from 12.7 to 82.1 μM), in comparison to ursolic acid (IC_{50} 26.6 μM. Compounds **120** and **127** displayed the strongest inhibitory activity (IC_{50} 12.7 and 13.5 μM, respectively) [49]. Five new polar pigments, talauxins E (**132**), I (**133**), L (**134**), Q (**135**), and V (**136**), along with the previously reported 9-demethyl FR-901235 (**55**), O-desmethylfunalenone (**100**), and duclauxin (**120**), were purified

from *Talaromyces stipitatus* (**Figure 14**). Talauxins are unusual heterodimers that are produced from the coupling of **120** with amino acids and are closely related to duclauxamide A (**119**), which was separated from *Penicillium manginii* [56]. They were fully characterized via spectroscopic and X-ray analysis. Compounds **120** and **132** exhibited weak cytotoxic effectiveness (IC_{50} 140 and 70 μM, respectively) versus NS-1 cells, compared to 5-fluorouracil (IC_{50} 4.6 μM) in the resazurin microplate assay, while **132** also had weak antibacterial potential versus *B. subtilis* (IC_{50} 265 μM), compared to clotrimazole (IC_{50} 0.4 μM) [43].

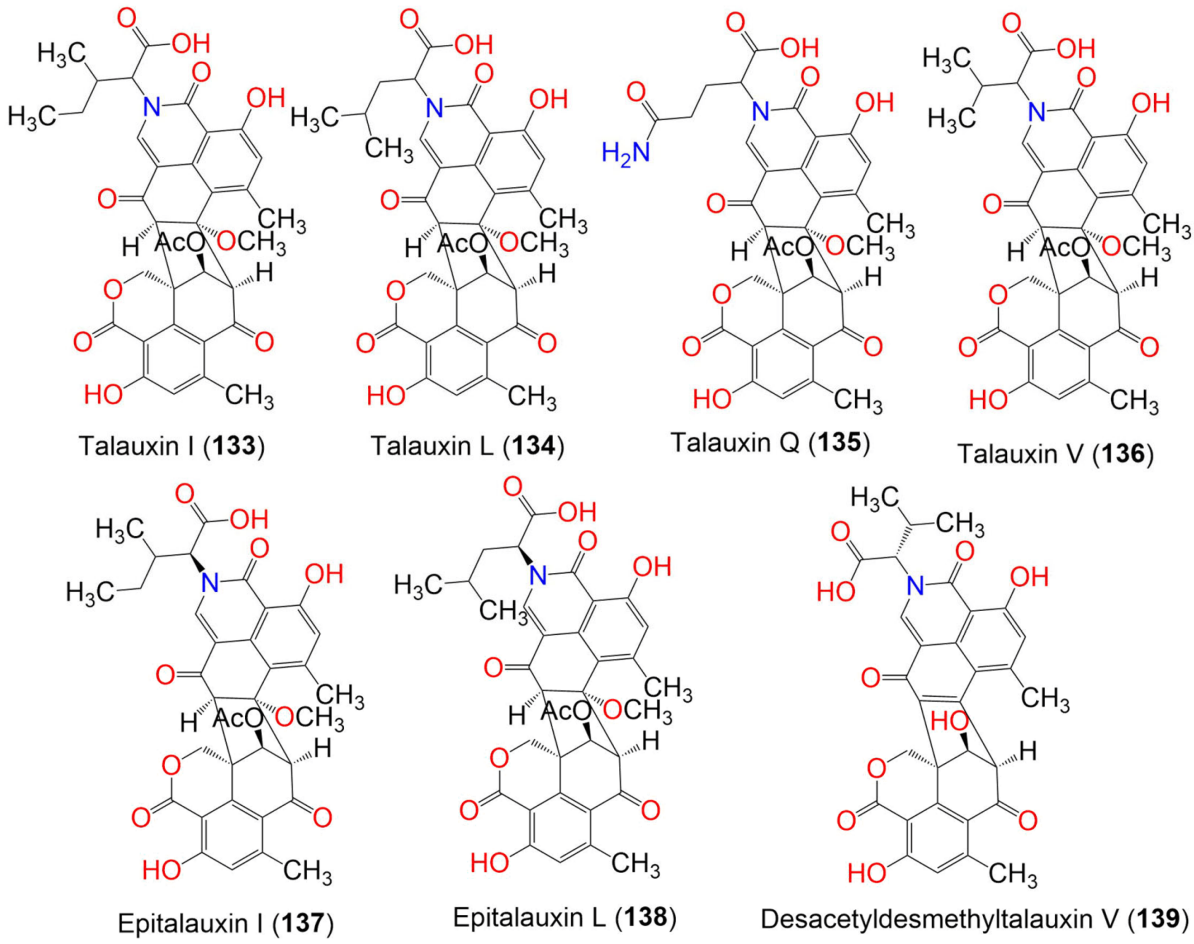

Figure 14. The structures of compounds **133**–**139**.

References

1. Ibrahim, S.R.M.; Altyar, A.E.; Mohamed, S.G.A.; Mohamed, G.A. Genus Thielavia: Phytochemicals, industrial importance and biological relevance. Nat. Prod. Res. 2021, 36, 5108–5123.
2. Ibrahim, S.R.M.; Mohamed, S.G.A.; Altyar, A.E.; Mohamed, G.A. Natural products of the fungal genus Humicola: Diversity, biological activity, and industrial importance. Curr. Microbiol. 2021, 78, 2488–2509.

3. Ibrahim, S.R.M.; Mohamed, S.G.A.; Sindi, I.A.; Mohamed, G.A. Biologically active secondary metabolites and biotechnological applications of species of the family Chaetomiaceae (Sordariales): An updated review from 2016 to 2021. Mycol. Prog. 2021, 20, 595–639.
4. Ibrahim, S.R.M.; Sirwi, A.; Eid, B.G.; Mohamed, S.G.A.; Mohamed, G.A. Bright Side of Fusarium oxysporum: Secondary Metabolites Bioactivities and Industrial Relevance in Biotechnology and Nanotechnology. J. Fungi. 2021, 7, 943.
5. Ibrahim, S.; Sirwi, A.; Eid, B.G.; Mohamed, S.; Mohamed, G.A. Fungal Depsides-Naturally Inspiring Molecules: Biosynthesis, Structural Characterization, and Biological Activities. Metabolites 2021, 11, 683.
6. Mohamed, G.A.; Ibrahim, S.R.M. Untapped Potential of Marine—Associated Cladosporium Species: An Overview on Secondary Metabolites, Biotechnological Relevance, and Biological Activities. Mar. Drugs. 2021, 19, 645.
7. Al-Rabia, M.W.; Mohamed, G.A.; Ibrahim, S.R.M.; Asfour, H.Z. Anti-inflammatory ergosterol derivatives from the endophytic fungus Fusarium chlamydosporium. Nat. Prod. Res. 2020, 35, 5011–5020.
8. Mohamed, G.A.; Ibrahim, S.R.M.; Alhakamy, N.A.; Aljohani, O.S. Fusaroxazin, a novel cytotoxic and antimicrobial xanthone derivative from Fusarium oxysporum. Nat. Prod. Res. 2020, 36, 952–960.
9. Mohamed, G.A.; Ibrahim, S.R.M.; El-Agamy, D.S.; Elsaed, W.M.; Sirwi, A.; Asfour, H.Z.; Koshak, A.E.; Elhady, S.S. Terretonin as a New Protective Agent against Sepsis-Induced Acute Lung Injury: Impact on SIRT1/Nrf2/NF-κBp65/NLRP3 Signaling. Biology 2021, 10, 1219.
10. Khayat, M.T.; Ibrahim, S.R.M.; Mohamed, G.A.; Abdallah, H.M. Anti-inflammatory metabolites from endophytic fungus Fusarium sp. Phytochem Lett. 2019, 29, 104–109.
11. Ibrahim, S.R.M.; Bagalagel, A.A.; Diri, R.M.; Noor, A.O.; Bakhsh, H.T.; Muhammad, Y.A.; Mohamed, G.A.; Omar, A.M. Exploring the activity of fungal phenalenone derivatives as potential CK2 inhibitors using computational methods. J. Fungi 2022, 8, 443.
12. Ibrahim, S.R.M.; Mohamed, G.A.; Al Haidari, R.A.; El-Kholy, A.A.; Zayed, M.F.; Khayat, M.T. Biologically active fungal depsidones: Chemistry, biosynthesis, structural characterization, and bioactivities. Fitoterapia 2018, 129, 317–365.
13. Hareeri, R.H.; Aldurdunji, M.M.; Abdallah, H.M.; Alqarni, A.A.; Mohamed, S.G.A.; Mohamed, G.A.; Ibrahim, S.R.M. Aspergillus ochraceus: Metabolites, bioactivities, biosynthesis, and biotechnological potential. Molecules 2022, 27, 6759.
14. Ibrahim, S.R.M.; Mohamed, G.A.; Khedr, A.M.I. γ-Butyrolactones from Aspergillus species: Structures, biosynthesis, and biological activities. Nat. Prod. Commun. 2017, 12, 791–800.

15. Ibrahim, S.R.M.; Abdallah, H.M.; Elkhayat, E.S.; Al Musayeib, N.M.; Asfour, H.Z.; Zayed, M.F.; Mohamed, G.A. Fusaripeptide A: New antifungal and anti-malarial cyclodepsipeptide from the endophytic fungus Fusarium sp. J. Asian Nat. Prod. Res. 2018, 20, 75–85.
16. Ibrahim, S.R.M.; Mohamed, G.A.; Al Haidari, R.A.; Zayed, M.F.; El-Kholy, A.A.; Elkhayat, E.S.; Ross, S.A. Fusarithioamide B, a new benzamide derivative from the endophytic fungus Fusarium chlamydosporium with potent cytotoxic and antimicrobial activities. Bioorg. Med. Chem. 2018, 26, 786–790.
17. Ibrahim, S.R.M.; Elkhayat, E.S.; Mohamed, G.A.; Fat'hi, S.M.; Ross, S.A. Fusarithioamide A, a new antimicrobial and cytotoxic benzamide derivative from the endophytic fungus Fusarium chlamydosporium. Biochem. Biophys. Res. Commun. 2016, 479, 211–216.
18. Ibrahim, S.R.; Abdallah, H.M.; Mohamed, G.A.; Ross, S.A. Integracides H–J: New tetracyclic triterpenoids from the endophytic fungus Fusarium sp. Fitoterapia 2016, 112, 161–167.
19. Ibrahim, S.R.; Mohamed, G.A.; Ross, S.A. Integracides F and G: New tetracyclic triterpenoids from the endophytic fungus Fusarium sp. Phytochem.Lett. 2016, 15, 125–130.
20. Nazir, M.; El Maddah, F.; Kehraus, S.; Egereva, E.; Piel, J.; Brachmann, A.O.; König, G.M. Phenalenones: Insight into the biosynthesis of polyketides from the marine alga-derived fungus Coniothyrium cereale. Org. Biomol. Chem. 2015, 13, 8071–8079.
21. Elsebai, M.F.; Saleem, M.; Tejesvi, M.V.; Kajula, M.; Mattila, S.; Mehiri, M.; Turpeinen, A.; Pirttilä, A.M. Fungal phenalenones: Chemistry, biology, biosynthesis and phylogeny. Nat. Prod. Rep. 2014, 31, 628–645.
22. Chooi, Y.H.; Tang, Y. Navigating the fungal polyketide chemical space: From genes to molecules. J. Org. Chem. 2012, 77, 9933–9953.
23. Song, R.; Feng, Y.; Wang, D.; Xu, Z.; Li, Z.; Shao, X. Phytoalexin phenalenone derivatives inactivate mosquito larvae and root-knot nematode as type-II photosensitizer. Sci. Rep. 2017, 7, 42058.
24. Hölscher, D.; Dhakshinamoorthy, S.; Alexandrov, T.; Becker, M.; Bretschneider, T.; Buerkert, A.; Crecelius, A.C.; De Waele, D.; Elsen, A.; Heckel, D.G.; et al. Phenalenone-type phytoalexins mediate resistance of banana plants (Musa spp.) to the burrowing nematode Radopholus similis. Proc. Natl. Acad. Sci. USA 2014, 111, 105–110.
25. Cooke, R.G.; Edwards, J.M. Naturally occurring phenalenones and related compounds. Fortschr. Chem. Org. Nat. 1981, 40, 153–190.
26. Harman, R.E.; Cason, J.; Stodola, F.H.; Adkins, A.L. Structural features of herqueinone, a red pigment from Penicillium herquei. J. Org. Chem. 1955, 20, 1260.

27. Munde, T.; Brand, S.; Hidalgo, W.; Maddula, R.K.; Svatoš, A.; Schneider, B. Biosynthesis of tetraoxygenated phenylphenalenones in Wachendorfia thyrsiflora. Phytochemistry 2013, 91, 165–176.
28. Bucher, G.; Bresolí-Obach, R.; Brosa, C.; Flors, C.; Luis, J.G.; Grillo, T.A.; Nonell, S. β-Phenyl quenching of 9-phenylphenalenones: A novel photocyclisation reaction with biological implications. Phys. Chem. Chem. Phys. 2014, 16, 18813–18820.
29. Phatangare, K.R.; Lanke, S.K.; Sekar, N. Phenalenone fluorophores-synthesis.; photophysical properties and DFT study. J. Fluoresc. 2014, 24, 1827–1840.
30. Lu, R.; Liu, X.; Gao, S.; Zhang, W.; Peng, F.; Hu, F.; Huang, B.; Chen, L.; Bao, G.; Li, C.; et al. New tyrosinase inhibitors from Paecilomyces gunnii. J. Agric. Food. Chem. 2014, 62, 11917–11923.
31. Rukachaisirikul, V.; Rungsaiwattana, N.; Klaiklay, S.; Phongpaichit, S.; Borwornwiriyapan, K.; Sakayaroj, J. γ-Butyrolactone.; cytochalasin.; cyclic carbonate.; eutypinic acid.; and phenalenone derivatives from the soil fungus Aspergillus sp. PSU-RSPG185. J. Nat. Prod. 2014, 77, 2375–2382.
32. Park, S.C.; Julianti, E.; Ahn, S.; Kim, D.; Lee, S.K.; Noh, M.; Oh, D.C.; Oh, K.B.; Shin, A.J. Phenalenones from a marine-derived fungus Penicillium sp. Mar. Drugs 2019, 17, 176.
33. Tansakul, C.; Rukachaisirikul, V.; Maha, A.; Kongprapan, T.; Phongpaichit, S.; Hutadilok-Towatana, N.; Borwornwiriyapan, K.; Sakayaroj, J. A new phenalenone derivative from the soil fungus Penicillium herquei PSU-RSPG93. Nat. Prod. Res. 2014, 28, 1718–1724.
34. Li, Q.; Zhu, R.; Yi, W.; Chai, W.; Zhang, Z.; Lian, X.-Y. Peniciphenalenins A–F from the culture of a marine-associated fungus Penicillium sp. ZZ901. Phytochemistry 2018, 152, 53–60.
35. Han, Y.; Sun, C.; Li, C.; Zhang, G.; Zhu, T.; Li, D.; Che, Q. Antibacterial phenalenone derivatives from marine-derived fungus Pleosporales sp. HDN1811400. Tetrahedron Lett. 2021, 68, 152938.
36. Intaraudom, C.; Nitthithanasilp, S.; Rachtawee, P.; Boonruangprapa, T.; Prabpai, S.; Kongsaeree, P.; Pittayakhajonwut, P. Phenalenone derivatives and the unusual tricyclic sesterterpene acid from the marine fungus Lophiostoma bipolare BCC25910. Phytochemistry 2015, 120, 19–27.
37. Macabeo, A.P.G.; Pilapil, L.A.E.; Garcia, K.Y.M.; Quimque, M.T.J.; Phukhamsakda, C.; Cruz, A.J.C.; Hyde, K.D.; Stadler, M. Alpha-glucosidase- and lipase-inhibitory phenalenones from a new species of pseudolophiostoma originating from Thailand. Molecules 2020, 25, 965.
38. Zhang, L.-H.; Feng, B.-M.; Sun, Y.; Wu, H.-H.; Li, S.-G.; Liu, B.; Liu, F.; Zhang, W.-Y.; Chen, G.; Bai, J.; et al. Flaviphenalenones A.–C, three new phenalenone derivatives from the fungus Aspergillus flavipes PJ03-11. Tetrahedron Lett. 2016, 57, 645–649.

39. Li, Y.; Yue, Q.; Jayanetti, D.R.; Swenson, D.C.; Bartholomeusz, G.A.; An, Z.; Gloer, J.B.; Bills, G.F. Anti-cryptococcus phenalenones and cyclic tetrapeptides from Auxarthron pseudauxarthron. J. Nat. Prod. 2017, 80, 2101–2109.
40. Gombodorj, S.; Yang, M.-H.; Shang, Z.-C.; Liu, R.-H.; Li, T.-X.; Yin, G.-P.; Kong, L.-Y. New phenalenone derivatives from Pinellia ternata tubers derived Aspergillus sp. Fitoterapia 2017, 120, 72–78.
41. Pang, X.; Zhao, J.Y.; Fang, X.M.; Zhang, T.; Zhang, D.W.; Liu, H.Y.; Su, J.; Cen, S.; Yu, L.Y. Metabolites from the plant endophytic fungus Aspergillus sp. CPCC 400735 and their anti-HIV activities. J. Nat. Prod. 2017, 80, 2595–2601.
42. Basnet, B.B.; Liu, L.; Zhao, W.; Liu, R.; Ma, K.; Bao, L.; Ren, J.; Wei, X.; Yu, H.; Wei, J.; et al. New 1,2-naphthoquinone-derived pigments from the mycobiont of lichen Trypethelium eluteriae Sprengel. Nat. Prod. Res. 2019, 33, 2044–2050.
43. Chaudhary, N.K.; Crombie, A.; Vuong, D.; Lacey, E.; Piggott, A.M.; Karuso, P. Talauxins: Hybrid phenalenone dimers from Talaromyces stipitatus. J. Nat. Prod. 2020, 83, 1051–1060.
44. Kim, D.C.; Minh Ha, T.; Sohn, J.H.; Yim, J.H.; Oh, H. Protein tyrosine phosphatase 1B inhibitors from a marine-derived fungal strain Aspergillus sp. SF-5929. Nat. Prod. Res. 2020, 34, 675–682.
45. Zhang, X.; Tan, X.; Li, Y.; Wang, Y.; Yu, M.; Qing, J.; Sun, B.; Niu, S.; Ding, G. Hispidulones A and B, two new phenalenone analogs from desert plant endophytic fungus Chaetosphaeronema hispidulum. J. Antibiot. 2020, 73, 56–59.
46. Yang, S.Q.; Mándi, A.; Li, X.M.; Liu, H.; Li, X.; Balázs Király, S.; Kurtán, T.; Wang, B.G. Separation and configurational assignment of stereoisomeric phenalenones from the marine mangrove-derived fungus Penicillium herquei MA-370. Bioorg. Chem. 2021, 106, 104477.
47. Yu, J.S.; Li, C.; Kwon, M.; Oh, T.; Lee, T.H.; Kim, D.H.; Ahn, J.S.; Ko, S.K.; Kim, C.S.; Cao, S.; et al. Herqueilenone, A, a unique rearranged benzoquinone-chromanone from the Hawaiian volcanic soil-associated fungal strain Penicillium herquei FT729. Bioorg. Chem. 2020, 105, 104397.
48. Wang, M.; Yang, L.; Feng, L.; Hu, F.; Zhang, F.; Ren, J.; Qiu, Y.; Wang, Z. Verruculosins A-B; new oligophenalenone dimers from the soft coral-derived fungus Talaromyces verruculosus. Mar. Drugs 2019, 17, 516.
49. Jiménez-Arreola, B.S.; Aguilar-Ramírez, E.; Cano-Sánchez, P.; Morales-Jiménez, J.; González-Andrade, M.; Medina-Franco, J.L.; Rivera-Chávez, J. Dimeric phenalenones from Talaromyces sp. (IQ-313) inhibit hPTP1B1-400: Insights into mechanistic kinetics from in vitro and in silico studies. Bioorg. Chem. 2020, 101, 103893.
50. Wu, B.; Ohlendorf, B.; Oesker, V.; Wiese, J.; Malien, S.; Schmaljohann, R.; Imhoff, J.F. Acetylcholinesterase inhibitors from a marine fungus Talaromyces sp. strain LF458. Mar. Biotechnol. 2015, 17, 110–119.

51. Zang, Y.; Genta-Jouve, G.; Escargueil, A.E.; Larsen, A.K.; Guedon, L.; Nay, B.; Prado, S. Antimicrobial oligophenalenone dimers from the soil fungus Talaromyces stipitatus. J. Nat. Prod. 2016, 79, 2991–2996.
52. Ernst-Russell, M.A.; Chai, C.L.L.; Elix, J.; McCarthy, P.M. Myeloconone A2, a new phenalenone from the lichen Myeloconis erumpens. Aust. J. Chem. 2000, 53, 1011–1013.
53. Lee, H.S.; Yu, J.S.; Kim, K.H.; Jeong, G.S. Diketoacetonylphenalenone, derived from Hawaiian volcanic soil-associated fungus Penicillium herquei FT729, regulates T Cell activation via nuclear factor-κB and mitogen-activated protein kinase pathway. Molecules 2020, 25, 5374.
54. Elsebai, M.F.; Ghabbour, H.A.; Mehiri, M. Unusual nitrogenous phenalenone derivatives from the marine-derived fungus Coniothyrium cereale. Molecules 2016, 21, 178.
55. Srinivasan, M.; Shanmugam, K.; Kedike, B.; Narayanan, S.; Shanmugam, S.; Gopalasamudram Neelakantan, H. Trypethelone and phenalenone derivatives isolated from the mycobiont culture of Trypethelium eluteriae Spreng and their anti-mycobacterial properties. Nat. Prod. Res. 2020, 34, 3320–3327.
56. Cao, P.; Yang, J.; Miao, C.P.; Yan, Y.; Ma, Y.T.; Li, X.N.; Zhao, L.X.; Huang, S.X. New duclauxamide from Penicillium manginii YIM PH30375 and structure revision of the duclauxin family. Org. Lett. 2015, 17, 1146–1149.